Finance and Economics Discussion Series

Federal Reserve Board, Washington, D.C.
ISSN 1936-2854 (Print)
ISSN 2767-3898 (Online)

Measuring Macroeconomic Stars: A Framework with Scarring Effects

Manuel Gonzalez-Astudillo, Jean-Philippe Laforte, Antoine Lepetit

2026-054

Please cite this paper as:
Gonzalez-Astudillo, Manuel, Jean-Philippe Laforte, and Antoine Lepetit (2026). "Measuring Macroeconomic Stars: A Framework with Scarring Effects," Finance and Economics Discussion Series 2026-054. Washington: Board of Governors of the Federal Reserve System, https://doi.org/10.17016/FEDS.2026.054.

Measuring Macroeconomic Stars: A Framework with Scarring Effects

Manuel González-Astudillo †1, Jean-Philippe Laforte ‡2, and Antoine Lepetit §3

[1]Federal Reserve Board, Washington, D.C., USA
[1]Escuela Superior Politécnica del Litoral, ESPOL, Guayaquil, Ecuador
[2]Federal Reserve Board, Washington, D.C., USA
[3]Federal Reserve Board, Washington, D.C., USA

June 29, 2026

Abstract

Potential output and the natural rate of unemployment are commonly estimated through trend-cycle decompositions, where they are identified as underlying trends reflecting slow-moving supply factors. In this paper, we extend this framework to accommodate the possibility that cyclical disturbances affect trends endogenously through "scarring" effects. Two major changes occur relative to standard specifications. First, a significant share of business-cycle fluctuations is absorbed by endogenous movements in the trends rather than shifts in the cycle. Second, the estimated cycle—relieved of explaining the persistence in real variables—tracks inflation developments more closely, including through a steeper Phillips curve. While this steeper slope implies a strong co-movement between inflation and real activity in response to cyclical shocks, such strong co-movement is rarely apparent in the data. Consequently, the estimation shows a shift toward more sizable changes in the purely supply-driven components of the trends, mirrored by smaller innovations in the cycle process. In turn, this rebalancing entails different historical paths for the activity gaps, carrying important implications for the conduct of monetary policy.

Keywords: potential output, natural rates, unobserved components model, Bayesian analysis, scarring

JEL Classification Numbers: C32, C34, E32

---

*The views expressed in this paper are solely the responsibility of the authors and should not be interpreted as reflecting the views of the Board of Governors of the Federal Reserve System.

†Email: manuel.p.gonzalez-astudillo@frb.gov

‡Email: jean-philippe.laforte@frb.gov

§Corresponding author. Email: antoine.lepetit@frb.gov

1 Introduction

Central bankers frequently reference starred variables to calibrate the stance of monetary policy. These "stars" represent an equilibrium state toward which macroeconomic variables, such as unemployment and output, are expected to converge once cyclical fluctuations have fully played out and the economy is expanding at its trend rate. Distinguishing whether economic fluctuations reflect slow-moving supply factors embodied in these stars or transitory supply and demand shocks is central to the appropriate policy response.

In practice, because these stars are latent or unobserved, economists rely on models to infer their values. Unobserved components (UC) models—time series frameworks that utilize macroeconomic theory to inform their empirical specification—are one of the leading methods of inference. These frameworks decompose macroeconomic time series into trends and cycles, treating the former as estimates of the stars. A widespread assumption underlying identification in UC models is that the trend factors are independent of the cyclical components. While this assumption is rooted in conventional macroeconomic theory, its validity has been increasingly challenged by the protracted recovery from the Global Financial Crisis (GFC) and a growing body of empirical evidence suggesting that demand shocks can exert persistent effects on real activity (see Ma and Zimmermann, 2023; Jorda, Singh and Taylor, 2020; Furlanetto et al., 2024, for example).

In this paper, we extend the workhorse UC model to accommodate the possibility that transitory or cyclical disturbances affect trends through a "scarring" mechanism. Our approach is informed by the core features of New Keynesian models with scarring effects, as established in Lepetit (2026). In these models, trends contain a purely supply-driven component—the stars—and a component that responds to cyclical shocks. While cyclical effects eventually fade, trends can deviate persistently from their supply-driven paths over the medium term. Another key feature of these models is a modified Phillips curve, which can be formulated in terms of the output gap relative to productive capacity (the joint demand- and supply-driven trend), or, alternatively, in terms of the level and *change* of the output gap relative to the purely supply-driven trend (the change component is often referred to as a *speed effect* in the Phillips curve). This second formulation is fundamental, as the relative weights on the level and speed effect terms reveal the extent of scarring in the data.

We incorporate these theoretical elements of scarring in a UC model and decompose output and unemployment into trends and cycles. Notably, we separately identify the purely supply-driven components of the trends—the stars—from the components capturing scarring effects. We estimate the model using U.S. data on real GDP, core PCE price inflation, the employment cost index (ECI) inflation rate, and the civilian unemployment rate from

1987:Q1 to 2024:Q4. To pin down the price inflation trend, we use survey-based measures of ten-year-ahead expectations of PCE price inflation, while the wage inflation trend is informed by the Congressional Budget Office's (CBO) estimate of trend labor productivity growth.

In describing our results, we contrast our model specification with an otherwise identical setup that does not allow for scarring, which we refer to as the "benchmark." Both are estimated on the *exact same* set of macroeconomic variables. Our results reveal that scarring effects are economically sizable, with the cyclical innovations contributing markedly to the formation of the estimated trends. Consequently, the output and unemployment trends in our framework exhibit significantly greater cyclicality and account for a larger portion of business-cycle fluctuations than those in the benchmark. The corollary to this finding is cyclical components that are markedly less volatile. Furthermore, our results show that the trend components driven by scarring effects now capture much of the "hump-shaped" dynamics of the macroeconomic variables conventionally attributed to the cycle. This shift in the dynamics is connected to changes in the parameters of the Phillips curves. As we noted earlier, our identification of the extent of scarring is based on the estimation of Phillips curves that include both level and speed terms; however, the Phillips curves of our model can also be expressed in a more traditional way as function of the relevant cycles—the deviations of output and unemployment from their respective overall trends. Given the reduced volatility of the cyclical process estimated under scarring, the slopes of the price and wage Phillips curves are four to five times larger than those estimated in the benchmark specification.

Our results also reveal a fundamental rebalancing in the drivers of macroeconomic fluctuations as identified by the two model specifications. Relative to the benchmark, the scarring specification attributes a larger share of the dynamics of the data to the supply-driven stars and less to cyclical innovations and cost-push shocks. This rebalancing occurs primarily because the scarring setup is better equipped than the benchmark specification to account for inflation developments through innovations to the cycle. The 1987-2024 sample period is generally characterized by weak co-movement between inflation and real activity, and by rapid shifts in inflation rather than slow, progressive buildups. With its lower cycle persistence and steeper Phillips curve, the scarring setup can more easily capture these swift variations in inflation through cyclical channels, and can do so without generating counterfactually large output changes. Consequently, it relies far less on cost-push factors than the benchmark case to explain inflation developments. However, the steeper Phillips curve slope also implies that the model can no longer rely as intensively as the benchmark specification on cyclical innovations to explain the bulk of real-side business-cycle fluctuations. If it did, the propagation of those shocks would generate large, counterfactual swings in inflation. Reconciling those swings with the actual inflation data would require introducing large, offsetting cost-push shocks, a possibility that is less statistically favored than the alternative of accounting for a greater share of the variance in real activity through movements in the supply-driven stars.

This rebalancing of volatility toward supply-driven stars has important implications for the conduct of monetary policy. Indeed, the greater prevalence of supply shocks directly affects the measurement of the activity gaps that monetary policymakers seek to stabilize—namely, the deviations of output and unemployment from their respective stars. We observe notable differences in these policy-relevant gaps during several key historical episodes. In 2008-2009, the scarring specification attributes an important role to adverse supply shocks, resulting in shallower output and unemployment gaps than the benchmark. Under scarring, the natural rate of unemployment rises to 7%, compared to 5% in the benchmark. Conversely, while the benchmark specification estimates a large, negative pre-pandemic unemployment gap of about -2%, the scarring setup reconciles the coexistence of below-target inflation and low unemployment via positive supply shocks, concluding that the labor market was roughly in balance at the time.

We establish that the scarring specification fits the data better, as demonstrated by a formal evaluation of the two setups using in-sample fit and (pseudo) out-of-sample forecasting metrics. We first perform a Bayesian model comparison exercise by calculating the Bayes factors through the Savage-Dickey density ratio, since the benchmark specification is nested in the scarring specification. We find that, under equal prior probabilities, the evidence is more than four times stronger for the scarring specification than the benchmark, implying that the scarring mechanism's superior fit of the data outweighs the penalty for its additional parameters. Moreover, forecasts produced from the sequential re-estimation of the two specifications over sub-samples of the data show the superior predictive capacity of the scarring alternative. Specifically, while the accuracy of price inflation forecasts is similar between specifications, the benchmark achieves this at the price of significantly worse performance in forecasting real activity and wage inflation. Overall, the various statistics used to assess the coherence of the specifications with the data support the importance and usefulness of the scarring mechanism.

Our paper contributes to the literature on UC models of macroeconomic trends and cycles. This literature originated with the univariate output decompositions of Watson (1986) and Clark (1987), and was extended to bivariate (e.g., Clark, 1989; Kuttner, 1994) and multivariate settings (e.g., Zaman, 2025; González-Astudillo and Laforte, 2025) for the estimation of macroeconomic stars. Most of this literature treats trends and cycles as distinct components, with trends capturing slow-moving supply forces and cycles capturing transitory fluctuations.

A smaller literature uses UC or state-space models to estimate hysteresis or scarring directly. Jaeger and Parkinson (1994) decompose unemployment into a natural rate and a cycle, allowing lagged cyclical unemployment to affect the natural rate. Related work extends this framework using richer dynamics, nonlinearities, and additional inflation, wage, or output information (e.g., Assarsson and Jansson, 1998; Logeay and Tober, 2006; Di Sanzo and Pérez-Alonso, 2011; Mossfeldt and Österholm, 2011; Bechný, 2019). Alichi et al. (2019) incorporate labor-market hysteresis into a multivariate filter for U.S. potential output, while Li and Mendieta-Muñoz (2024) introduce dynamic UC hysteresis models in which output gaps affect potential output through lagged effects.

Closest to our identification strategy is Calvert Jump and Stockhammer (2023), who derive an ARIMAX representation from a reduced-form Phillips curve and use inflation-unemployment dynamics to identify the degree of unemployment hysteresis. We share their insight that Phillips-curve restrictions help identify hysteresis. Our contribution is to embed this insight in a structural New Keynesian model with history-dependent productive capacity and to estimate the implied restrictions in a multivariate UC framework. This allows us to identify scarring in both output and unemployment through price and wage Phillips curves, while separately measuring supply-driven stars and the endogenous scarring components of productive and labor-market capacity.

The paper is organized as follows. Section 2 presents the theoretical framework that guides the specification of the UC model of Section 3. Section 4 describes the data and estimation approach. Section 5 presents our main results; specifically, it contrasts our scarring specification with the benchmark setup. Section 6 compares the in-sample fit and out-of-sample forecasting performance of the two specifications. Finally, Section 7 concludes.

2 Theoretical framework

The framework in this section follows Lepetit (2026), who demonstrates that several structural models embedding the possibility that demand shocks might temporarily or permanently scar the productive capacity of the economy—including the insider-outsider model of Galí (2022), the endogenous growth model of Queralto (2022), and the heterogeneous firms model of Baqaee, Farhi and Sangani (2024)—can be nested within a common log-linear system. This system, referred to as the four-equation New Keynesian model with scarring, is defined as follows:

$$y_t - y_t^* = E_t y_{t+1} - E_t y_{t+1}^* - \left(i_t - E_t \pi_{t+1} - r_t^*\right), \tag{1}$$

$$\pi_t = \beta E_t \pi_{t+1} + \kappa \left(y_t - \tilde{y}_t^*\right) + \varepsilon_t^s, \tag{2}$$

$$i_t = \phi_\pi \pi_t, \tag{3}$$

$$\tilde{y}_t^* = \underbrace{y_t^*}_{\text{supply shocks}} + \underbrace{\omega \sum_{j=1}^{J} \delta^j \left(y_{t-j} - y_{t-j}^*\right)}_{\text{scarring effects}}. \tag{4}$$

In these equations, π_t denotes the inflation rate, y_t output, i_t the policy rate, and E_t the rational expectations operator conditional on information available in period t. The variables r_t^* and y_t^* represent the real interest rate and output levels that would prevail under flexible prices. While y_t^* is driven exclusively by supply-side factors such as technology or labor supply shocks, r_t^* may also be influenced by demand disturbances, such as preference shocks. Finally, ε_t^s is a cost-push shock.

The primary departure from the standard New Keynesian model is that the Phillips curve in (2) depends on "productive capacity," $\tilde{y}_t^*$, rather than the purely supply-driven potential, y_t^*. The law of motion of $\tilde{y}_t^*$ in (4) specifies that current productive capacity depends on contemporaneous supply forces as well as the scars left by past cyclical disturbances, which are captured by past deviations of output from its supply-driven potential.

By substituting (4) in (2), the Phillips curve can be reformulated in terms of the deviation of output from its purely supply-driven potential, y_t^*. In this specification, both the level of the output gap and its current and past changes influence inflation dynamics:

$$\pi_t = \beta E_t \pi_{t+1} + \kappa \left(1 - \omega \sum_{j=1}^{J} \delta^j\right) (y_t - y_t^*) + \kappa\omega \sum_{i=0}^{J-1} \sum_{j=i+1}^{J} \delta^j \Delta \left(y_{t-i} - y_{t-i}^*\right) + \varepsilon_t^s. \tag{5}$$

The coefficients attached to the different output gap terms on the right hand side of this equation are directly informative about the dynamics of productive capacity, $\tilde{y}_t^*$. We distinguish three specific cases based on these parameters. First, the independence case arises if $\omega = 0$ or $\delta = 0$. Under this parameterization, productive capacity is independent of demand factors and only the level of the output gap appears in (5). This is the standard case considered in the literature. Second, the temporary scarring case arises when both $\omega, \delta > 0$ and $\omega \sum_{j=1}^{J} \delta^j < 1$. Under this parameterization, demand shocks have persistent, albeit ultimately temporary, effects on productive capacity, and both the level of the $y_t - y_t^*$ gap and its current and past changes appear in (5). Third, the hysteresis case arises when $\omega \sum_{j=1}^{J} \delta^j = 1$. Under this parameterization, demand shocks have permanent effects on productive capacity and only changes in the $y_t - y_t^*$ gap drive inflation.

This analytical framework provides two main insights for our empirical analysis. First, it allows for a decomposition of the overall output trend—productive capacity—into a purely supply-driven component and a component responsive to cyclical fluctuations. Second, it suggests that the Phillips curve can be formulated either in terms of the gap relative to productive capacity or in terms of the level and the change of the gap relative to the supply-driven trend. In the latter formulation, the relative weights attached to the level and change terms reveal the extent of scarring effects. These insights guide the specification of the unobserved components model in the following section.

3 An Unobserved Components Model with Scarring or Hysteresis

The basic structure of our UC model with scarring or hysteresis begins with a set of features that have become standard in the literature on the estimation of UC models of the business cycle, going all the way back to Watson (1986) and Clark (1987). We start with the GDP-price inflation block, which we formulate by following closely the theoretical framework described in Section 2. Then, we add an unemployment rate-wage inflation block as past research has shown that the unemployment rate provides important information about the cyclical position of the economy (see for example González-Astudillo and Roberts, 2022).

3.1 Price Inflation and Output

We specify the inflation process with a hybrid Phillips curve in which inflation expectations are treated as a latent variable specified as a weighted average of trend inflation, denoted as π_t^*, and actual lagged inflation (see Basistha and Nelson, 2007). As in our theoretical model, inflation also depends both on the gap between (log) output y_t and its supply-driven trend, y_t^*, and the change in that gap (we assume that $J = 1$ for simplicity):

$$\pi_t = \beta\pi_{t-1} + (1-\beta)\pi_t^* + \kappa_1(y_t - y_t^*) + \kappa_2\Delta(y_t - y_t^*) + \varepsilon_t^\pi, \tag{6}$$

with $\beta \in [0, 1)$, $\kappa_1, \kappa_2 \geq 0, \kappa_1 + \kappa_2 > 0$ and $\varepsilon_t^\pi \sim N(0, \sigma^2_{\varepsilon^\pi})$. Unlike in the theoretical model, which does not account for trend inflation, we impose that the coefficients on lagged inflation and trend inflation sum to one such that there is no long-run trade-off between inflation and output.

As is common in the UC literature, we assume that the supply-driven output trend, y_t^*, follows a local-linear trend specification, as follows:

$$y_t^* = \mu_{t-1} + y_{t-1}^* + \eta_t^{y^*}, \tag{7}$$

$$\mu_t = \mu_{t-1} + \eta_t^{\mu}, \tag{8}$$

where $\eta_t^{y^*} \sim N(0, \sigma^2_{\eta^{y^*}})$ and $\eta_t^{\mu} \sim N(0, \sigma^2_{\eta^{\mu}})$.

Productive capacity, $\tilde{y}_t^*$, is instead defined as the output trend that results from both supply and demand influences. The cycle, $\tilde{c}_t$, is defined as the deviation from that trend:

$$y_t = \tilde{y}_t^* + \tilde{c}_t, \tag{9}$$

$$\tilde{c}_t = \phi_1 \tilde{c}_{t-1} + \phi_2 \tilde{c}_{t-2} + \varepsilon_t, \tag{10}$$

with ϕ_1 and ϕ_2 satisfying stationarity conditions and $\varepsilon_t \sim N(0, \sigma^2_{\varepsilon})$. The dynamic link between the two output trends, y_t^* and $\tilde{y}_t^*$ is given by the following equation, which is the mirror image of (4) in the theoretical model:

$$\tilde{y}_t^* = y_t^* + \delta^y \left(y_{t-1} - y_{t-1}^* \right), \tag{11}$$

where $\delta^y \equiv \kappa_2 / \left(\kappa_1 + \kappa_2 \right)$. When $\kappa_2 = 0$, we have the standard UC model of trend-cycle decomposition of output, which is nested in our specification; we refer to that model as the benchmark specification. When $\kappa_1 = 0$, we have a UC model with hysteresis. In all other cases, we have a UC model with temporary scarring.[1] Moreover, we can verify that combining (6) and (11) delivers a Phillips curve expressed in terms of the cyclical component $\tilde{c}_t$:

$$\pi_t = \beta \pi_{t-1} + (1 - \beta) \pi_t^* + \left(\kappa_1 + \kappa_2 \right) \tilde{c}_t + \varepsilon_t^{\pi}, \tag{12}$$

with $\varepsilon_t^{\pi} \sim N(0, \sigma^2_{\varepsilon^{\pi}})$.

We close this block of the model with the equations that characterize trend inflation. We assume trend inflation evolves according to a random walk process (see Stock and Watson, 2007; Aruoba and Schorfheide, 2011; Cogley and Sargent, 2015; Mertens, 2016, for example):

$$\pi_t^* = \pi_{t-1}^* + \eta_t^{\pi^*},$$

[1] To see this more clearly, note that (11) can be written as

$$\tilde{y}_t^* = y_t^* + w_t^y,$$

for $w_t^y \equiv \delta^y \left(y_{t-1} - y_{t-1}^* \right)$, where it can be shown that

$$w_t^y = \rho^y w_{t-1}^y + \delta^y \tilde{c}_{t-1},$$

with $\rho^y = \delta^y$. Therefore, when $\kappa_1, \kappa_2 > 0$, w_t^y is a stationary process and deviations of $\tilde{y}_t^*$ from y_t^* are only transitory (temporary scarring), whereas, when $\kappa_1 = 0$, w_t^y contains a unit root and deviations of $\tilde{y}_t^*$ from y_t^* are permanent (hysteresis). When $\kappa_2 = 0$, we have that $\tilde{y}_t^* = y_t^*$ $\forall t$, i.e., the benchmark UC model.

where $\eta_t^{\pi^*} \sim N(0, \sigma^2_{\pi^*})$. Moreover, in a similar fashion to Del Negro, Giannoni and Schorfheide (2015), Bauer and Rudebusch (2020), and González-Astudillo and Laforte (2025) we use information on 10-year-ahead inflation expectations, denoted as π_t^e, to pin down the inflation trend:

$$\pi_t^e = \pi_t^* + e_t,$$

where $e_t \sim N(0, \sigma_e^2)$.

3.2 Wage Inflation and Unemployment Rate

We also allow for the possibility of scarring effects in unemployment. To do so, we apply the same logic as in the previous subsection and specify a Phillips curve for wage inflation, π_t^w, with both level and acceleration terms, as follows:

$$\pi_t^w = \lambda + \beta^w \pi_{t-1}^w + (1 - \beta^w)(g_t^* + \pi_t^*) + \gamma_1(u_t - u_t^*) + \gamma_2 \Delta(u_t - u_t^*) + \varepsilon_t^{\pi^w}, \tag{13}$$

with $\beta^w \in [0, 1), \gamma_1 < 0, \gamma_2 \leq 0$, $\varepsilon_t^{\pi^w} \sim N(0, \sigma^2_{\varepsilon^{\pi^w}})$, and where g_t^* is trend labor productivity in period t, u_t is the unemployment rate in period t, and u_t^* is its supply-driven trend. We allow for a wedge, λ, between wage inflation and the sum of the labor productivity and inflation trends, $g_t^* + \pi_t^*$, to account for the declining labor share over our sample. Trend labor productivity is informed by data on a measure of trend labor productivity, g_t, as follows:

$$\begin{aligned} g_t &= g_t^* + v_t, \\ g_t^* &= g_{t-1}^* + \eta_t^{g^*}, \end{aligned}$$

where $v_t \sim N(0, \sigma_v^2)$ and $\eta_t^{g^*} \sim$ i.i.d. $N(0, \sigma^2_{\eta^{g^*}})$.

The supply-driven unemployment trend, u_t^*, evolves according to a unit-root process:

$$u_t^* = u_{t-1}^* + \eta_t^{u^*}, \tag{14}$$

where $\eta_t^{u^*} \sim N(0, \sigma^2_{\eta^{u^*}})$. We also define an unemployment trend $\tilde{u}_t^*$ that is driven by both supply and demand factors. The two unemployment trends are related by the following equation

$$\tilde{u}_t^* = u_t^* + \delta^u(u_{t-1} - u_{t-1}^*), \tag{15}$$

with $\delta^u = \gamma_2 / (\gamma_1 + \gamma_2)$.[2] As was the case with output, we can check that combining equa-

[2] In line with findings in the literature (see Reifschneider, Wascher and Wilcox, 2015; Furlanetto et al., 2024), we do not allow for hysteresis effects in unemployment; indeed, we assume that γ_1 is strictly negative. There could, however, be temporary scarring effects if $\gamma_2 < 0$. Similar to the output specification, we can

tions (13) and (15) delivers a wage Phillips curve expressed in terms of the $u_t - \tilde{u}_t^*$ gap:

$$\pi_t^w = \lambda + \beta^w \pi_{t-1}^w + (1-\beta^w)(g_t^* + \pi_t^*) + (\gamma_1 + \gamma_2)(u_t - \tilde{u}_t^*) + \varepsilon_t^{\pi^w}, \tag{16}$$

with $\varepsilon_t^{\pi^w} \sim N(0, \sigma^2_{\varepsilon^{\pi^w}})$.

Finally, we impose an Okun's law relationship that relates the deviations of unemployment and output from their respective trends:

$$u_t = \tilde{u}_t^* + \theta_1 \tilde{c}_t + \theta_2 \tilde{c}_t + \upsilon_t, \tag{17}$$

where $\theta_1, \theta_2 < 0$ and $\upsilon_t \sim N(0, \sigma_\upsilon^2)$ is an Okun's law error.

3.3 Adding Stochastic Volatility and Outliers' Treatment

We make our model specification robust to changes in the volatility of the shocks over time and we allow for outliers to account for the sequence of extreme observations recorded during the COVID-19 pandemic. Not allowing for these possibilities in the data would deliver less efficient (and perhaps incorrect) estimates than otherwise.

We incorporate stochastic volatility in each of the error terms of our model under a random walk log-volatility process. Our outliers in the observable variables are additive and follow a contaminated (location-shift) normal distribution.[3]

3.4 A Note on Identification

We ensure that the coefficients of our model setup are globally identified through the introduction of the inflation equation, (6), which features both level and speed terms. These terms allow us to identify κ_1 and κ_2 which in turn uniquely determine the output scarring/hysteresis coefficient, $\delta^y = \frac{\kappa_2}{\kappa_1 + \kappa_2}$.

write

$$\tilde{u}_t^* = u_t^* + w_t^u,$$

for $w_t^u \equiv \delta^u \left(u_{t-1} - u_{t-1}^*\right)$, where it can be shown that

$$w_t^u = \rho^u w_{t-1}^u + \delta^u \left(u_{t-1} - \tilde{u}_{t-1}^*\right),$$

with $\rho^u = \delta^u$. Therefore, when $\gamma_2 < 0$, w_t^u is a stationary process and deviations of $\tilde{u}_t^*$ from u_t^* are only transitory (temporary scarring). When $\gamma_2 = 0$, we have that $\tilde{u}_t^* = u_t^*$ $\forall t$, i.e., the benchmark UC model.

[3]In the case of stochastic volatility, we assume that each error term, say ξ_t, is as follows: $\xi_t = \exp(0.5h_t)\epsilon_t$, where $\epsilon_t \sim$ i.i.d. $N(0,1)$, $h_t = h_{t-1} + u_t$, $u_t \sim$ i.i.d. $N(0, \sigma_u^2)$, and $h_0 \sim N(\mu_0, \sigma_0^2)$. In turn, for outliers, we assume that each observable variable, say x_t, has a probability density function given by $f(x_t|\mu, \sigma^2, \delta, o_t) = (1-\delta)\phi(x_t|\mu, \sigma^2) + \delta\phi(x_t|\mu + o_t, \sigma^2)$, where μ is the conditional mean of x_t with information up to period $t-1$ and σ^2 is its variance. $\phi(x|\mu, \sigma^2)$ is the normal probability density with mean μ and variance σ^2 whereas $\delta \in [0,1]$. Here, o_t is the location shifting factor that constitutes our outliers.

Alternatively, one could estimate a UC model with scarring or hysteresis such as the one implied by equations (7)-(11) using data on output alone. In that case, although the necessary order condition for identification is satisfied (see Li and Mendieta-Muñoz, 2024), the sufficient rank condition is not. Because δ^y enters the reduced-form representation of the model nonlinearly, it is impossible to uniquely identify it globally unless one assumes $\delta^y = 1$. In Appendix B, we present the formal proof of this global underidentification problem and demonstrate how incorporating inflation data via a Phillips curve with speed effects resolves it.

4 Data and Estimation Approach

We use U.S. data on real GDP, the civilian unemployment rate, the price deflator for PCE excluding food and energy, the 10-year ahead inflation expectations of the PCE price deflator used in the FRB/US model (available as "PTR" in the public FRB/US package, a mnemonic that we will use henceforth), the employment cost index, and the Congressional Budget Office (CBO) estimate of trend labor productivity growth.[4] All the variables come from the Federal Reserve Economic Data (FRED) database of the Federal Reserve Bank of St. Louis, except PTR and trend labor productivity growth, which come from the publicly available database of FRB/US and the January 2025 release of the historical data and economic projections of the CBO, respectively.

Our empirical analysis focuses on the period from 1987:Q1 to 2024:Q4. While the existing literature suggests that scarring or hysteresis effects are detectable in data spanning from the 1980s onward, these effects appear less prevalent in earlier samples (see Benati and Lubik, 2022; Furlanetto et al., 2024). Given that our model—while accounting for stochastic volatility—assumes time-invariant parameters, it is not explicitly designed to capture structural shifts in the extent of scarring.[5] We therefore restrict our attention to this recent period to ensure a more homogeneous sample for the estimation of our key parameters.

We estimate the model with Bayesian methods. The Gibbs sampler alternates sampling between coefficients and latent states drawn with the Durbin and Koopman (2002) simulation smoother. The stochastic volatility processes are estimated with the Kim, Shephard and Chib (1998) approach whereas additive outliers in the observation equations of the UC model are

[4]The FRB/US model is a large-scale estimated general equilibrium model of the U.S. economy that has been in use at the Federal Reserve Board since 1996. The model is designed for detailed analysis of monetary and fiscal policies. More details can be found at the following webpage: `https://www.federalreserve.gov/econres/us-models-about.htm`

[5]For a similar argument within the context of vector autoregression models, see Bianchi, Nicolò and Song (2023)

estimated with the Verdinelli and Wasserman (1991) approach.

Table 1 reports information about the prior distributions used for the estimation in column 2. The hyperparameters of the prior distributions associated with the parameters of output, the unemployment rate, and the inflation rate are informed by the results in González-Astudillo and Laforte (2025). In turn, the hyperparameters of the prior distributions of the wage inflation equation are informed by the results in Glick, Leduc and Pepper (2022). Notice that, under the prior distributions, there is no scarring or hysteresis, on average, as both κ_2 and γ_2 are centered at zero. The means of the prior distributions of the initial values of the nonstationary latent factors are set in accordance with the initial values of the relevant variables in the sample.[6]

5 Estimation Results and Analysis

In this section, we compare the estimation results of our model setup that incorporates scarring effects (the 'scarring specification') with those of an otherwise standard UC model that enforces the independence hypothesis (the 'benchmark specification').[7]

5.1 Parameter estimates

Table 1 reports key estimation results about the posterior distribution of the parameters for both specifications. Columns 3 and 4 show the results for the benchmark while columns 5 and 6 show the results for scarring.

The posterior mean estimates of the speed coefficients, κ_2 and γ_2, are 0.28 and -0.31, respectively, and their distributions are away from the zero parametrization that corresponds to the benchmark specification. These estimates imply posterior means of the scarring coefficients, δ^y and δ^u, which can be interpreted as the degree of history dependence in productive and labor market capacities, equal to 0.58 and 0.47, respectively. These magnitudes are consistent with a persistent (but not extremely) scarring mechanism at play for both real activity variables.

[6] For the stochastic volatility processes, our prior hyperparementers are informed by the posterior distribution moments in González-Astudillo and Laforte (2025), except for the volatilities of the error terms of the wage inflation and trend labor productivity growth equations. For these variables, we inform the prior hyperparameters with results from simple linear regressions on these variables, using estimates from the public FRB/US database as latent variables (namely, u_t^*). For the outliers processes, δ has a Beta$(0.005, 0.995)$ prior distribution and $o_t \sim N(0, 100 \times \text{MSE})$, where MSE is the mean-squared error of observable variable x_t's one-step-ahead forecast obtained with the UC model under the means of the prior distributions.

[7] Since the scarring specification is preferred over the hysteresis specification (see the model comparisons in Section 6), we relegate the discussion of the results of the hysteresis specification to Appendix E.

Table 1: Prior Distributions and Estimation Results

		Benchmark		Scarring	
	Prior Dist.	Post. Mean	68% CI	Post. Mean	68% CI
ϕ_1	N(1.5,1)	1.74	[1.67,1.81]	1.25	[1.02,1.48]
ϕ_2	N(-0.6,1)	-0.75	[-0.83,-0.68]	-0.30	[-0.52,-0.09]
θ_1	N(-0.35,0.25)	-0.30	[-0.43,-0.17]	-0.35	[-0.51,-0.19]
θ_2	N(-0.20,0.25)	-0.42	[-0.53,-0.30]	-0.47	[-0.61,-0.33]
β	N(0.7,0.5)	0.57	[0.49,0.66]	0.49	[0.38,0.61]
κ_1	N(0.1,0.5)	0.09	[0.06,0.12]	0.19	[0.08,0.31]
κ_2	N(0,0.5)	0	—	0.28	[0.10,0.46]
λ	N(-0.2,1)	-0.59	[-0.72,-0.46]	-0.65	[-0.79,-0.52]
β^w	N(0.8,0.5)	0.40	[0.31,0.49]	0.34	[0.23,0.46]
γ_1	N(-0.1,0.5)	-0.15	[-0.21,-0.10]	-0.36	[-0.61,-0.14]
γ_2	N(0,0.5)	0	—	-0.31	[-0.53,-0.09]
y_0^*	N(911.9,5)	911.9	[910.9,913.3]	911.9	[910.5,913.5]
μ_0	N(1,1)	0.76	[0.62,0.89]	0.74	[0.61,0.88]
π_0^*	N(5,2)	4.88	[4.74,5.02]	4.88	[4.74,5.03]
u_0^*	N(5.9,2)	4.87	[4.09,5.60]	5.22	[4.50,5.93]
g_0^*	N(1.8,1)	1.77	[1.70,1.84]	1.77	[1.70,1.84]
κ		0.09	[0.06,0.12]	0.48	[0.23,0.71]
γ		-0.15	[-0.21,-0.10]	-0.67	[-0.99,-0.32]
$\rho^y = \delta^y$		0	—	0.58	[0.35,0.79]
$\rho^u = \delta^u$		0	—	0.47	[0.21,0.71]

Note: "N" stands for normal distribution. The first parameter is the mean and the second is the standard deviation.

One major shift that occurs because of the presence of scarring is found in the features of the cycle process. The estimated cyclical component is substantially more persistent in the benchmark specification. At the posterior means, the AR(2) roots of the cycle are approximately 0.95 and 0.79 in the benchmark, compared with 0.93 and 0.32 under scarring. Thus, while both specifications imply a highly persistent dominant root, the benchmark cycle is closer to a unit-root process and also features a second root that contributes materially to propagation. By contrast, the scarring specification sharply reduces the second root, making the cycle behave much more like a lower-persistence AR(1) process. The implication is that, under scarring, the model no longer needs the cycle to carry the persistence of output and unemployment fluctuations as much as in the benchmark.

The second most noticeable difference between the estimates of the two specifications lies in the Phillips curve coefficients. The parameters governing inflation inertia, β and β^w, are somewhat lower in the scarring specification than in the benchmark, but the main distinction is in the estimated slopes of the price and wage Phillips curves. The benchmark implies a relatively weak link between real activity and inflation, consistent with other findings in this literature (see González-Astudillo and Laforte, 2025; Zaman, 2025, for example). In particular, the price Phillips curve slope, κ, has a posterior mean estimate equal to 0.09, while that of the wage Phillips curve slope, γ, is -0.15. In contrast, the scarring specification yields posterior mean estimates for these slopes—which are now related to the gaps relative to productive and labor-market capacities—that are four to five times larger (0.48 for κ and -0.67 for γ).

5.2 The Scarring Mechanism

What accounts for these differences in the Phillips curves, particularly the much larger slopes under scarring? To answer this question, we return to the cycle process and examine its propagation to output and unemployment under both specifications. Figure 1 shows the responses to a one percent increase in the level of output through an innovation in the cycle for each specification. While both specifications generate hump-shaped output and unemployment responses, comparing the top panels in Figures 1a and 1b reveals a stark divergence in the underlying transmission channels. In the scarring specification, the hump-shaped profile is achieved by relying on the endogenous response of productive capacity, w_t^y (orange bars), in addition to the dynamics of the cycle, $\tilde{c}_t$ (blue bars). In the benchmark, by contrast, this profile is achieved solely through the pronounced persistence of the cycle process, c_t (blue bars). Moreover, under scarring, the overall effects on output and unemployment peak sooner and decay toward the steady state more rapidly than in the benchmark specification.

This difference in propagation has implications for how inflation is related to the degree of economic slack in each specification. Because the benchmark setup explains business cycle fluctuations in real activity solely through shifts in the cycle while the scarring specification attributes these fluctuations to a combination of cyclical shifts and pro-cyclical movements in productivity capacity, the cycle is naturally smaller in amplitude under scarring. Given that the cyclical components enter the Phillips curves isomorphically in both specifications, mapping a smaller cycle to the same observed inflation dynamics mechanically yields a larger slope estimate in the scarring specification. Put differently, ignoring the possibility that cyclical shocks may affect productive capacity leads one to overstate the size of the cycle, resulting in a downward bias in traditional estimates of the Phillips curve slope (Lepetit, 2026). A direct implication of this higher degree of association between inflation dynamics and economic slack is that the responses of price and wage inflation to the same cyclical shock are larger and more front-loaded under scarring, as can be seen in the bottom two panels of Figures 1a and 1b.

These structural differences documented above are reflected in the estimated historical paths of the model's latent processes. Figures 2 and 3 show that the trends $\tilde{y}_t^*$ and $\tilde{u}_t^*$ in the scarring specification (orange-dashed lines)—which internalize persistent contributions from past cyclical developments—exhibit much more pronounced short-term dynamics than the benchmark trends, y_t^* and u_t^* (blue-dotted lines), which are driven solely by exogenous supply-side factors. As a direct consequence of the trends absorbing a greater share of medium-run fluctuations in the scarring model, the remaining cyclical component exhibits significantly lower volatility than its benchmark counterpart. This is visible in Figure 4, which compares the cycle in the benchmark specification, c_t (blue-dotted lines), with that estimated under scarring, $\tilde{c}_t$ (orange-dashed lines).

Figure 2 also shows that the estimated purely supply-driven trend under scarring, y_t^* (green-dashed-dotted line), periodically decouples from its benchmark counterpart (the blue-dotted line), most prominently during the GFC. Analogously, the purely supply-driven unemployment trends diverge across the two specifications during the GFC and the late 2010s, as shown in Figure 3 (green-dashed-dotted line versus blue-dotted line). While the comparison of the $y_t - y_t^*$ gap in the benchmark specification to the gap $y_t - \tilde{y}_t^*$ in the scarring specification is the relevant one to explain inflation dynamics, the comparison of the $y_t - y_t^*$ gaps between the two specifications is more consequential for the design of monetary policy, as we discuss in more detail below.

Figure 1: Impulse-response Analysis

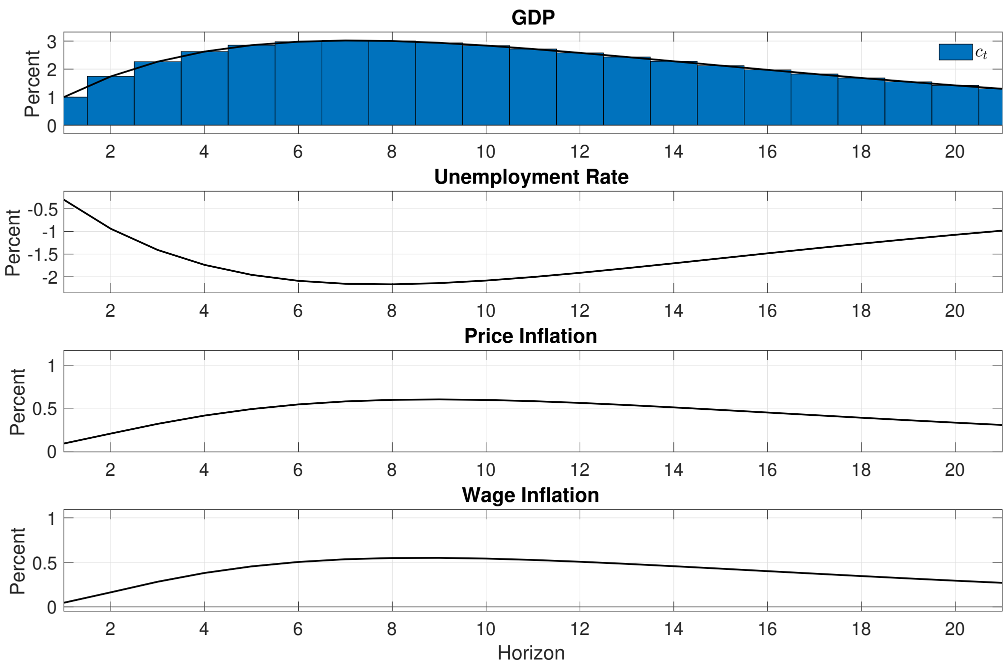

(a) Benchmark

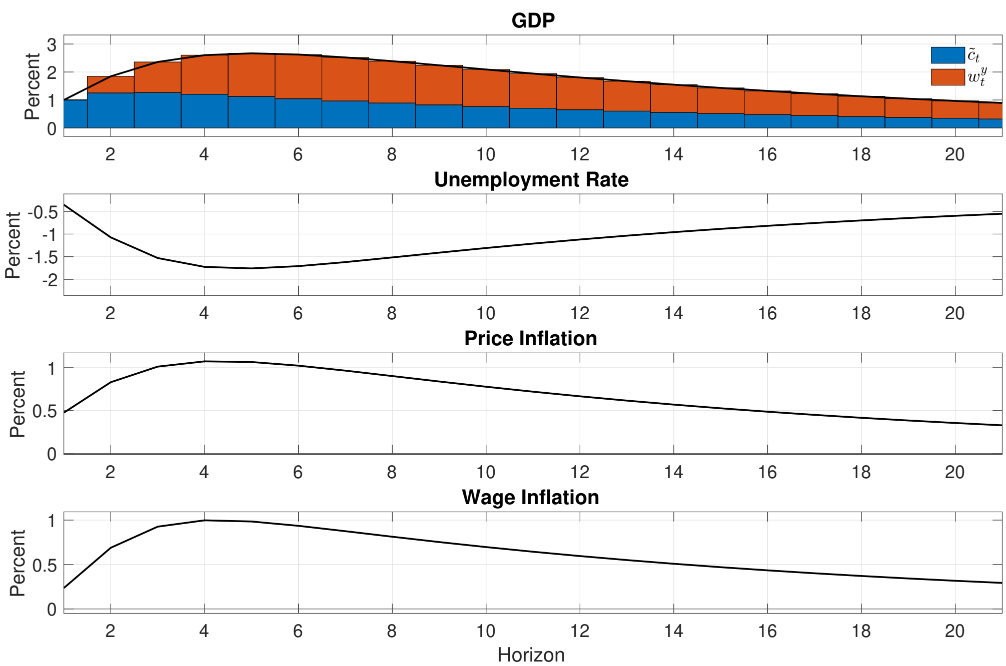

(b) Scarring

Note: Responses to a one-time shock to ε_t that increases GDP by one percent on impact.

Figure 2: Trend Output

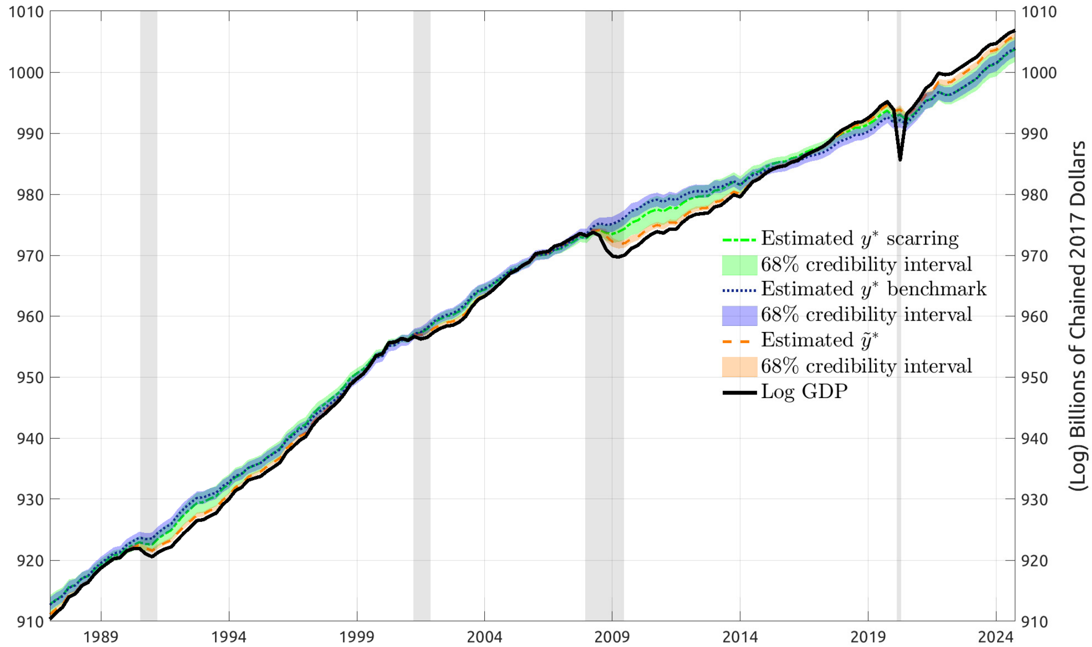

Figure 3: Trend Unemployment

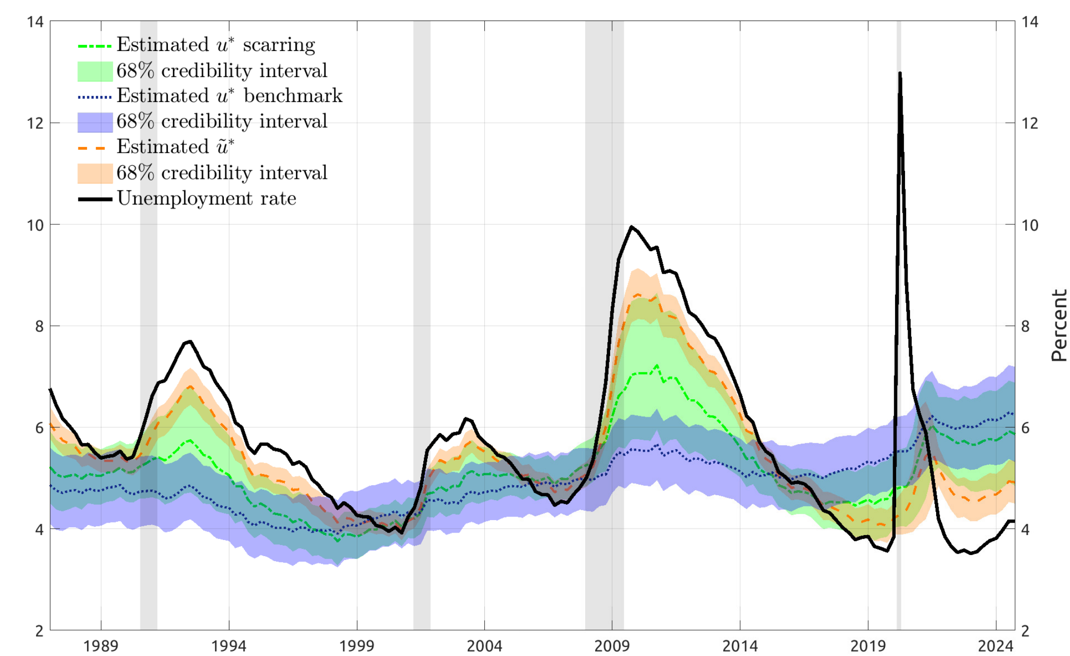

Figure 4: Output Gap

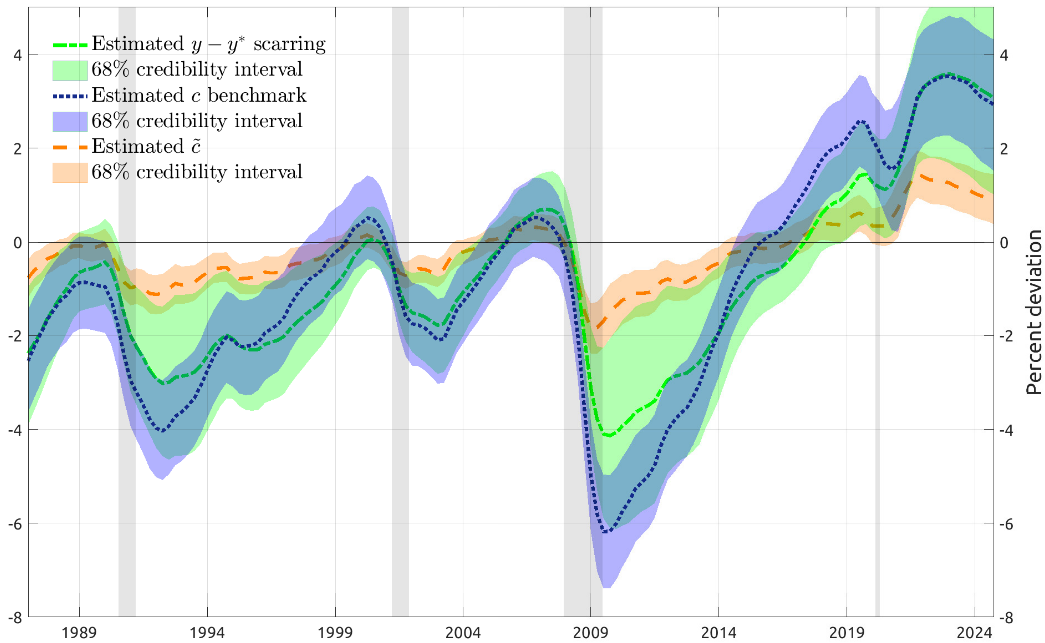

5.3 The Rebalancing

Our results reveal a fundamental shift in the types of shocks needed to explain the data. As shown in Figure 5, comparing the dashed-orange to the blue-dotted lines, the shocks driving the supply-driven trends for output and unemployment (η^{y^*}, η^{μ}, and η^{u^*}) become more volatile under scarring. Meanwhile, shocks to the cycle (ε) and cost-push shocks (ε^{π} and ε^{π^w}) become less volatile. As we explain next, this rebalancing happens because the two specifications face different constraints when trying to match the same historical data.

To understand the forces driving this rebalancing, it is instructive to examine the trade-offs involved in fitting business-cycle co-movements. In general, structural innovations to the cycle represent an appealing mechanism to fit the data, especially when unexpected variations in real activity and inflation move in the same direction, for instance when the economy experiences aggregate demand shocks. Under the benchmark specification, because the estimated Phillips curve is flat, this implies that any attempt to fit an observed shift in inflation solely through cyclical channels requires engineering a counterfactually large change in output.

This first problem is made worse by a mismatch in timing. Because the cycle is highly persistent and hump-shaped in the benchmark specification (see Figure 1), it cannot easily

Figure 5: Stochastic Volatilities

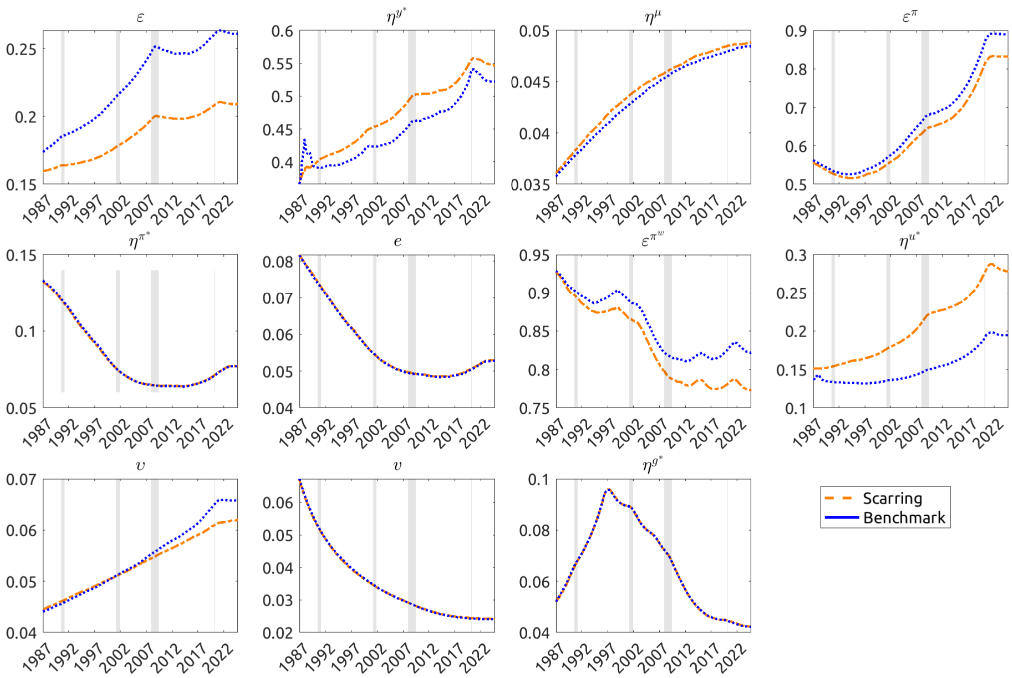

capture sudden, short-lived shifts in inflation—such as the sharp, temporary disinflation during the 2008-2009 crisis—without creating a long-lasting buildup in inflation in subsequent periods. In our sample, such progressive, persistent buildups are not prevalent, and shifts in inflation are generally not accompanied by very large output swings. For those reasons, the estimation limits its use of cyclical shocks and instead relies heavily on cost-push shocks to fit inflation. This reliance is clearly reflected in the upper panel of Figure 6, which presents the historical decomposition of price inflation.

The introduction of the scarring mechanism changes the nature of the constraints faced by the model. In the scarring specification, a cyclical shock still triggers highly persistent, hump-shaped dynamics in output, but the cycle itself reacts more rapidly and decays much faster than under the benchmark. As we discussed earlier, this shift occurs because the medium-run persistence of real variables is now successfully absorbed by endogenous movements in the trends rather than by the cycle itself. We also noted that a direct consequence of this decoupling between the forces driving business-cycle fluctuations in real activity (the joint contributions of the cycle and scarring effects) and those driving inflation (only the cycle) is that the Phillips curve is steeper under scarring.

Because the cycle is no longer required to capture the medium-run persistence in real activity, it becomes a far more efficient tool for explaining the inflation data. Its rapid reaction

Figure 6: Price Inflation Shock Decomposition

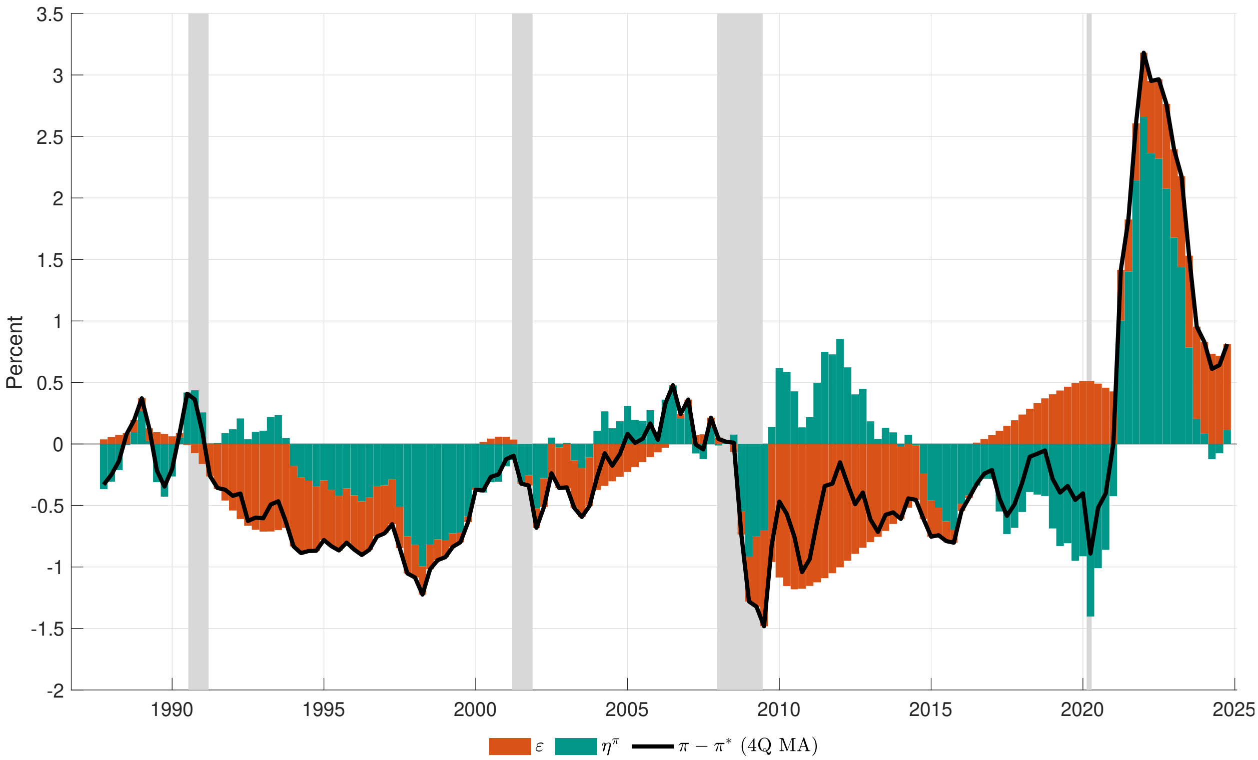

(a) Benchmark

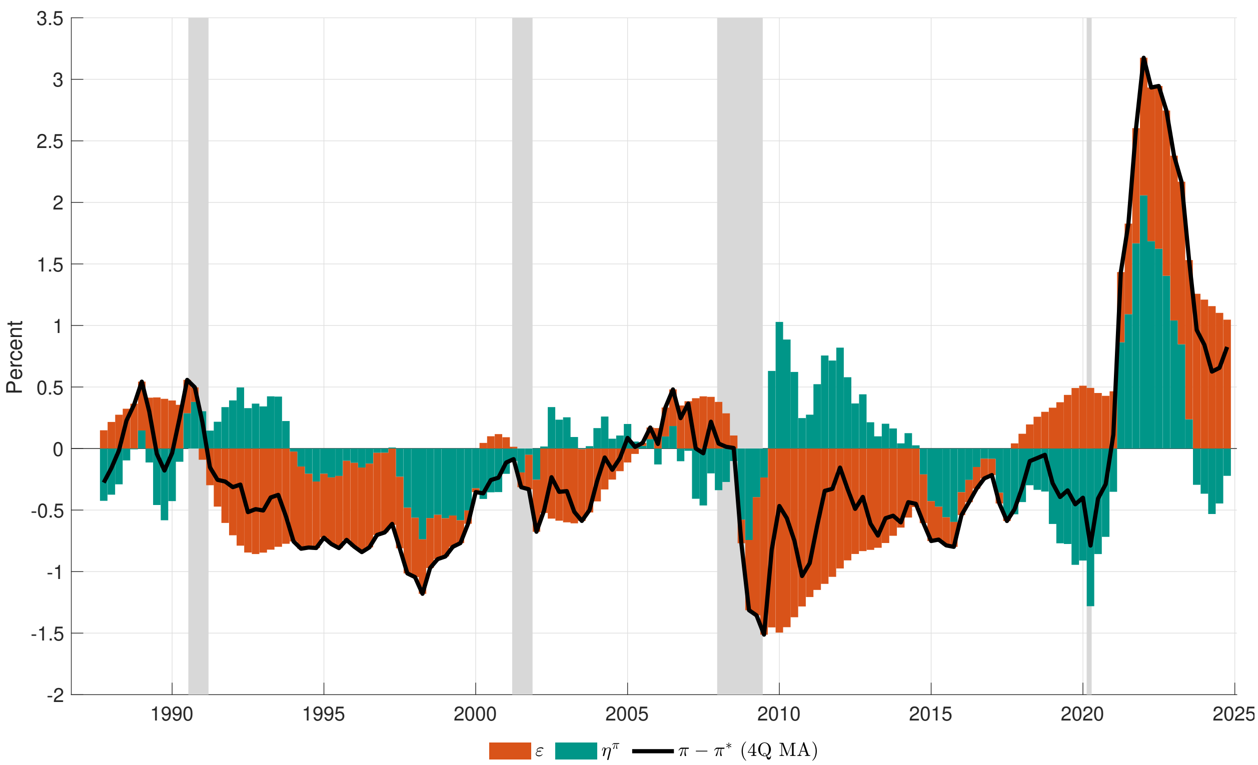

(b) Scarring

Note: Shock decompositions obtained at the posterior mean estimates. The black line corresponds to the difference between the inflation data and the contribution from the state of the Kalman filter's initial conditions and the trend inflation process.

allows it to account for swift shifts in inflation, while the steeper Phillips curve ensures it can do so without generating an implausibly large output response. These dynamics explain why the historical decomposition of inflation in the bottom panel of Figure 6 shows a more prominent role for cyclical shocks and a diminished reliance on cost-push factors compared with the benchmark case.

However, the steeper Phillips curve slope under scarring implies that the model can no longer rely heavily on cyclical innovations to explain the bulk of real-side business-cycle fluctuations. If cyclical shocks were utilized as intensively as they are in the benchmark specification, their propagation through the steep Phillips curve would generate massive, counterfactual swings in inflation. Reconciling those swings with the data would force the model to introduce large, offsetting cost-push shocks—a parameterization that is highly inefficient from a forecast-error minimization perspective.

Instead, to explain the smooth, persistent variations in output and unemployment without destabilizing inflation, the model forces other innovations to pick up the slack. It shifts the variance away from the cycle and toward the purely supply-driven trend shocks, allowing macroeconomic stars to account for a much larger share of fluctuations in real activity.

5.4 Implications for the measurement of activity gaps

The rebalancing of volatility from cyclical shocks and cost-push factors toward supply-driven trends carries significant implications for monetary policy. Indeed, the greater prevalence of supply shocks directly affects the measurement of the activity gaps, $y_t - y_t^*$ and $u_t - u_t^*$. From a welfare perspective, these are the fundamental margins that monetary policymakers should attempt to close in addition to stabilizing inflation.[8]

We observe notable differences in these policy-relevant gaps during two distinct historical episodes: the GFC and the expansionary years preceding the pandemic. In 2008–2009, because the drop in price and wage inflation was relatively small compared to the historic collapse in real activity, the scarring specification attributes an important role to adverse supply shocks. Consequently, the estimate of the natural rate of unemployment rises to about 7% under scarring, compared to just 5% in the benchmark specification (green-dashed-dotted line versus blue-dashed line in Figure 3). Conversely, in 2018–2019, the scarring specification reconciles the coexistence of below-target inflation with solid output growth and low unemployment by relying on positive supply shocks (the contribution of those supply

[8]This section focuses on the measurement of activity gaps, but the presence of scarring also carries other implications for the design of optimal monetary policy. In particular, introducing speed effects in the Phillips curve alters the dynamic trade-off between inflation stabilization and the stabilization of the $y_t - y_t^*$ gap. Moreover, with scarring, policymakers may want to assign a larger relative weight to the stabilization of real activity (Galí, 2022).

shocks is shown by the yellow bars in the unemployment shock decomposition of Figure D.2b in Appendix D). This channel results in significantly shallower output and unemployment gaps than those inferred by the benchmark model.

To inform their policy decisions, central bankers often attempt to infer the position of these activity gaps from observed movements in inflation and real activity, using models conceptually similar to our benchmark specification. In this regard, a striking and problematic feature of the benchmark specification is that price and wage inflation play almost no role in determining the trajectory of potential output, y_t^*, as shown in the top panel of Figure 7: the blue bars, that represent the contribution from output and unemployment rate data, explain virtually all the variation in the estimate of y_t^*.

In contrast, the scarring specification gives a much greater role to price and wage inflation data in informing the path of the estimate of y_t^*, as can be seen in the bottom panel of Figure 7. Indeed, the scarring framework features a much tighter connection between inflation and the cycle, which is embodied in the steeper Phillips curves. Consequently, when a large swing in output or unemployment fails to trigger a corresponding shift in inflation, the model interprets this nominal stability as a clear signal that the change in real activity is driven by persistent supply shocks rather than cyclical shifts.

6 Model Evaluation

In this section, we provide metrics to determine whether the introduction of the scarring mechanism is favored by the data. To that end, we take two approaches. First, we evaluate the in-sample model fit of our proposed specification. Second, we assess its out-of-sample forecasting performance.

6.1 In-sample model evaluation

To establish which specification is preferred by the data, we perform a Bayesian model comparison between the two setups we have presented so far. We denote with M_s the specification with scarring and with M_b, the benchmark specification. The Bayes factor is as follows, assuming $P(M_s) = P(M_b) = 0.5$:

$$BF_{s:b} = \frac{p(\text{data}|M_s)}{p(\text{data}|M_b)}.$$

Because M_b is nested in M_s (when $\kappa_2 = \gamma_2 = 0$) and the prior distributions of the models' parameters are independent, the Bayes factor can be computed with the Savage-

Figure 7: Data decomposition of y^*

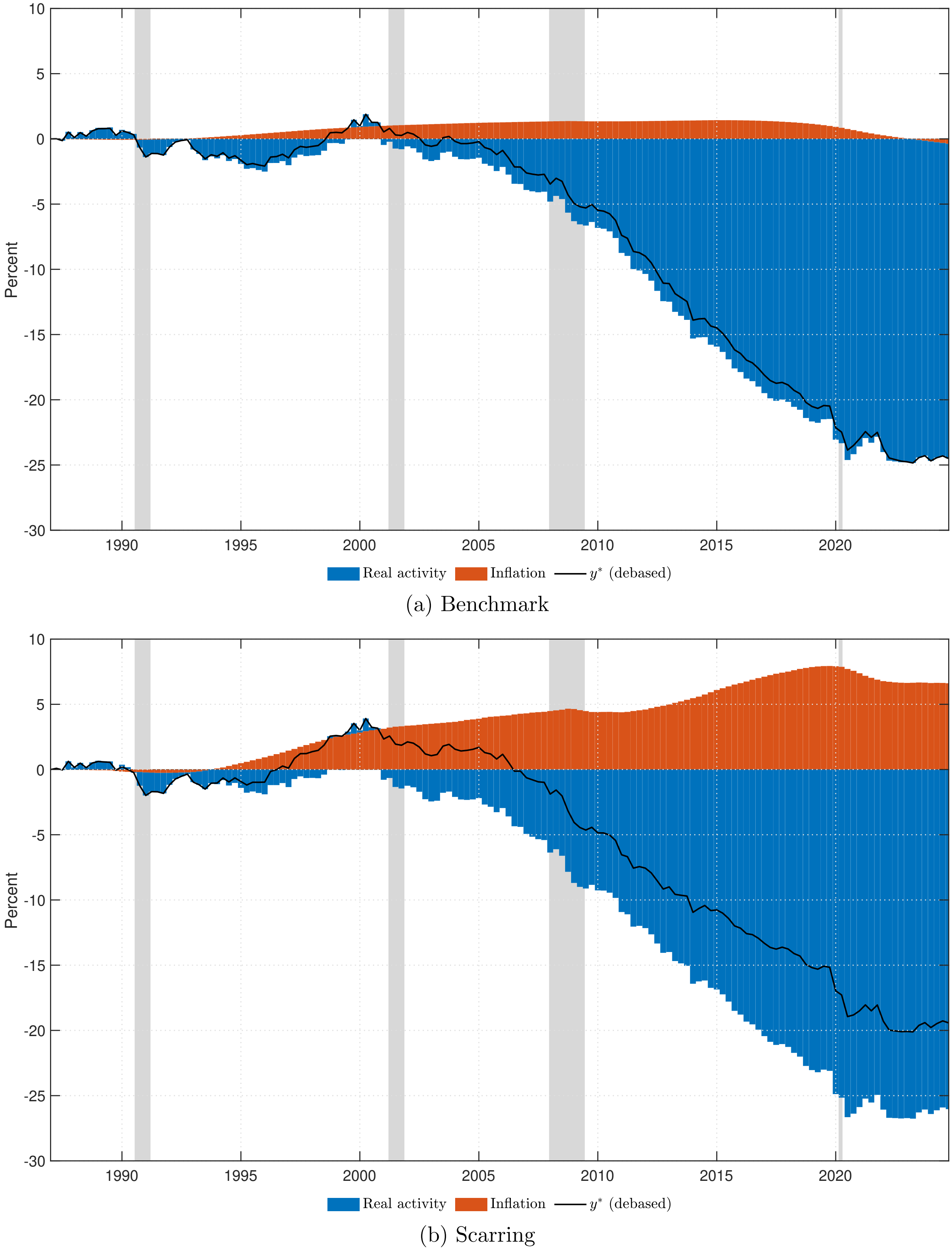

(a) Benchmark

(b) Scarring

Note: "Debased" means that the contribution of the model's initial conditions has been removed. The plotted series therefore shows the part of y_t^* explained by the observed data. The real activity component combines the contributions from the GDP, unemployment rate and trend productivity growth data. The inflation component combines the price inflation, wage inflation and long-run inflation expectations data.

Dickey density ratio, as follows:

$$BF_{s:b} = \frac{p(\kappa_2 = 0|M_s)p(\gamma_2 = 0|M_s)}{p(\kappa_2 = \gamma_2 = 0|\text{data}, M_s)},$$

and we can calculate $P(M_s|\text{data}) = \frac{BF_{s:b}}{1+BF_{s:b}}$.

Figure 8 shows the results of the Bayesian model comparison between the benchmark and scarring specifications. The figure plots a contour of the joint posterior density of κ_2 and γ_2 where the peak of the density (around 5.5) is in the yellow area. This joint density evaluated at the point $\kappa_2 = \gamma_2 = 0$ (the left uppermost point) reaches a value around 0.5 whereas the joint prior distribution evaluated at $\kappa_2 = \gamma_2 = 0$ (not shown in the figure) is about 2.5. Consequently, the Bayes factor is close to 5, meaning that the probability of the model with scarring, given the data, is above 0.8.

Moreover, Figure 9 shows the prior and posterior distribution densities to evaluate if the data favor a model with scarring, individually on output (Figure 9a) or the unemployment rate (Figure 9b). In the first case, the Bayes factor is computed as $BF_{s(\kappa_2=0):b} = \frac{p(\kappa_2=0|M_s)}{p(\kappa_2=0|\text{data},M_s)}$, which allows us to obtain the probability of a model with scarring in output only, given the data. In the second case, the Bayes factor is $BF_{s(\gamma_2=0):b} = \frac{p(\gamma_2=0|M_s)}{p(\gamma_2=0|\text{data},M_s)}$, which gives the probability of a model with scarring in unemployment only, given the data. In both cases, there is strong evidence of output or unemployment scarring against a model specification without any of these mechanisms. We interpret our in-sample evaluation exercise as being in favor of the scarring specification.[9]

6.2 Out-of-sample forecasting performance

The model comparison exercise based on the marginal likelihood assesses the performance of the specifications by summarizing their in-sample fit while balancing for parsimony given the data. However, the specifications can also be assessed for their out-of-sample predictive accuracy, which may differ from their in-sample counterpart, especially if a model fits history well but extrapolates poorly. Also, in-sample measures are derived solely on one-step ahead predictions from the models. The out-of-sample exercise allows us to evaluate and compare the forecasting performance of the model for longer-horizon projections. In this section, we conduct pseudo real-time forecasting exercises to investigate further whether relaxing

[9]The Bayesian approach penalizes additional parameters unless they help improve the probability to observe the data given the richer model. The scarring specification increases the odds of the data with a combination of two counteracting forces. First, it reduces the volatility of the cycle without sacrificing its effect on the amplitude and persistence of output (thanks to the scarring mechanism), which is a gain for the model. Second, it increases the volatility of the purely supply-driven shocks, which is detrimental for the model. The first effect counteracts the second.

Figure 8: Bayesian Model Comparison

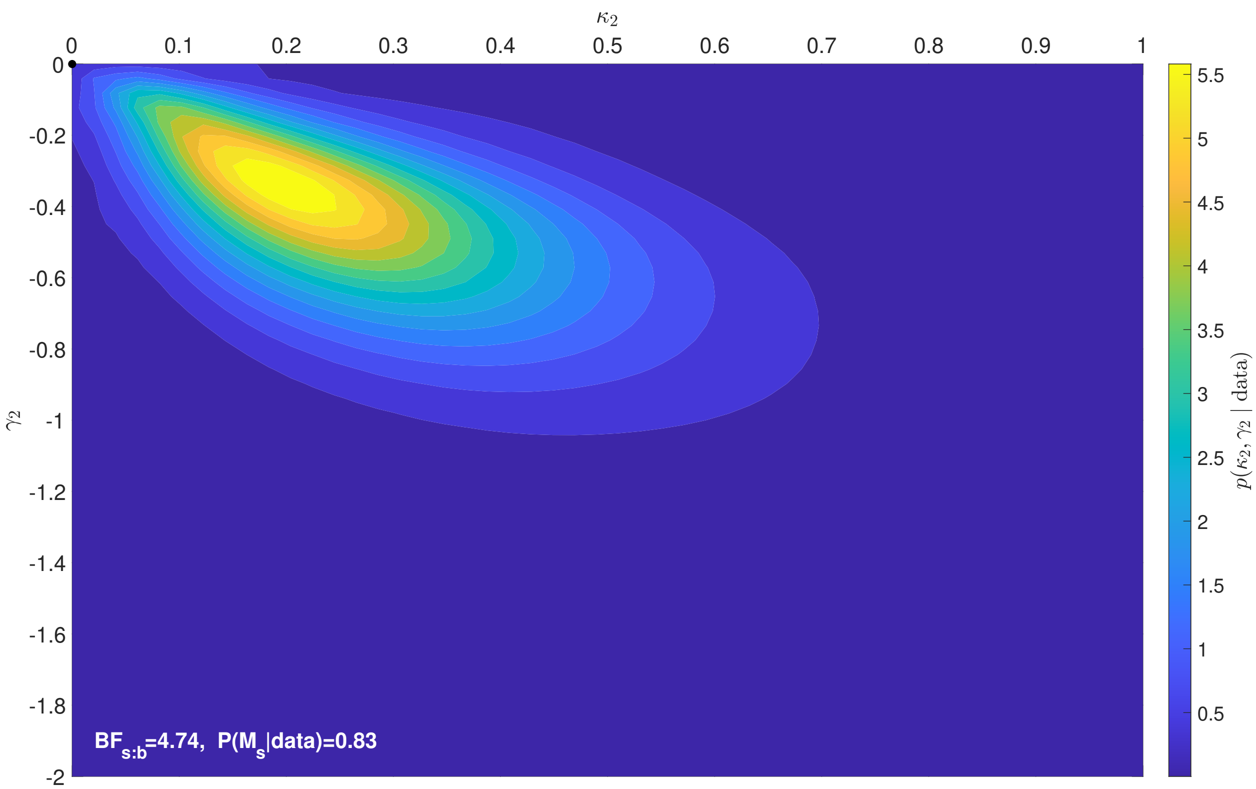

Figure 9: Savage-Dickey Density Ratios

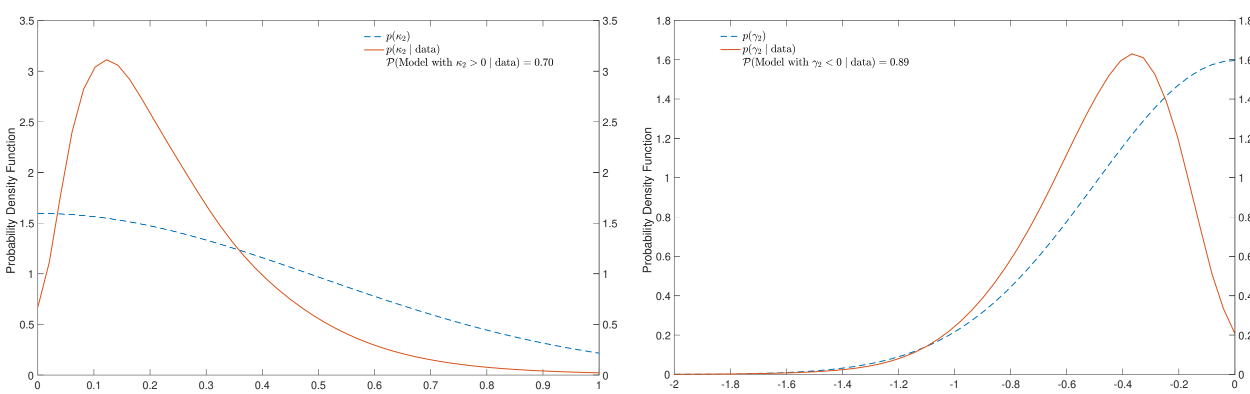

(a) Test of a model without scarring in output

(b) Test of a model without scarring in unemployment the independence assumption improves the UC model's ability to forecast real activity and inflation measures.

In our forecasting performance comparison, we consider the benchmark, scarring, and hysteresis specifications. We initially estimate each specification with a sample that starts in 1987:Q1 and ends in 1998:Q4. We then sequentially re-estimate each specification with a sample that is augmented by one quarter at the time, until the estimation for the 1986:Q1-2024:Q4 sample is reached. With each sample and for each model specification, we produce one- and four-quarter ahead forecasts of the price and wage inflation rates as well as the level of GDP and the unemployment rate.[10]

We report the forecasting performance of each model specification according to two statistics: the traditional root mean squared errors (RMSEs) and the continuous ranked probability score (CRPS) (see Gneiting and Raftery, 2007). By taking both parameter and variable state uncertainty on board, the CRPS statistic evaluates the performance of the predictive distribution of forecasts rather than that of a single and representative prediction (as, for instance, the case of the RMSE statistic). The CRPS penalizes not only the bias but also the dispersion implied by the predictive distribution. We also perform the Diebold and Mariano (1995) (DM) test for each pair of RMSEs' specifications (benchmark and hysteresis) relative to the scarring setup.

Table 2 reports the ratios of the RMSE and CRPS of the benchmark and hysteresis specifications relative to those of the scarring specification for the forecast horizons of one and four quarters ahead.

Both statistics tell a common story and support the results discussed in Section 6.1. The scarring specification dominates more often than not the benchmark and hysteresis specifications. Focusing on the RMSE statistics, the scarring specification outperforms the benchmark for all variables except the inflation process, for which the differences in performances are not statistically significant. The dominance of the scarring specification over the benchmark is more evident at the shorter horizon. For all variables, except price inflation, the reduction in the variance of the forecast errors is statistically significant at either the one or ten percent levels of significance, according to the DM test. The performances of the scarring and hysteresis specifications are much closer: there are no statistical differences between the two specifications, except for the unemployment rate where the scarring setup outperforms hysteresis at the five percent level of significance.

While the benchmark and scarring specifications forecast price inflation equally well, the

[10] We did not include the hysteresis specification in the in-sample comparison exercise because nesting it in the scarring specification may induce undesirable behavior of the Savage-Dickey density ratio. This could occur because the hysteresis specification induces a unit root in the process w_t^y. In any case, results of the in-sample fit tests still favor the scarring specification over hysteresis.

Table 2: Forecast evaluation (1999–2024)

		Benchmark		Hysteresis	
		1Q	4Q	1Q	4Q
Inflation	RMSE	1.01	0.99	1.00	0.99
	CRPS	1.02	0.97	1.00	0.99
Unemployment Rate	RMSE	1.06***	1.17**	1.02**	1.01
	CRPS	1.30	1.31	1.03	0.99
Wage Inflation	RMSE	1.10**	1.06	1.01	1.00
	CRPS	1.11	1.10	1.01	1.01
Real GDP (level)	RMSE	1.03*	1.23*	1.03	1.14
	CRPS	1.05	1.31	1.01	1.12

Note: RMSE denotes root-mean-square error. CRPS denotes continuous rank probability score. 1Q and 4Q denote one and four quarters ahead, respectively. The table reports each statistic relative to scarring, so a number greater than one means the statistic reported is larger than the corresponding statistic of the scarring specification. *,** ,*** denotes 10%, 5%, and 1% significance, respectively, of the Diebold and Mariano (1995) test of equality of forecasting performance between the model specification in the table and the scarring's.

benchmark's comparable performance comes at the expense of worse predictive accuracy for all other variables, as shown in Table 2. As documented in Section 5, any contribution from cyclical innovations to inflation in the benchmark specification simultaneously entails a persistent response in real variables that conflicts with the observed data. The benchmark can only account for moderately persistent movements in the inflation gap by inducing larger (because of a flatter Philips curve) and much longer-lasting dynamics in output and the unemployment rate than what the data would require. In contrast, the scarring specification possesses the flexibility to explain inflation dynamics through movements in the cyclical gap without degrading its forecast accuracy for real economic activity.

All told, both in-sample fit and out-of-sample forecasting evaluations favor the scarring specification over the benchmark, as the former provides an additional channel that allows the model to account for the same movements in inflation with significantly smaller innovations and lesser repercussions on the real side of the economy that are not warranted by the dynamics implied by the data.

7 Conclusion

This paper extends the standard UC framework used to estimate macroeconomic stars by allowing cyclical disturbances to affect trend components endogenously through scarring effects. The model distinguishes between supply-driven stars and broader measures of productive and labor-market capacity that also incorporate the persistent effects of past cyclical conditions. This distinction is central for both identification and interpretation: price and wage Phillips-curve restrictions discipline the extent of scarring, while the separation between supply-driven trends, the stars, and scarring components allows the model to assess whether persistent movements in real activity reflect supply-side developments or the endogenous propagation of past cyclical shocks.

Our results show that scarring effects are economically sizable. Relative to an otherwise identical benchmark specification, the scarring model assigns a larger role to endogenous movements in productive and labor-market capacity and a smaller role to the cycle itself. As a result, the estimated cycles are less volatile and less persistent, while the scarring components absorb much of the hump-shaped dynamics in output and unemployment that standard UC models attribute to highly persistent cyclical fluctuations. Because the inflation-relevant gaps are smaller under scarring, the estimated price and wage Phillips-curve slopes are substantially larger than in the benchmark. The model therefore recovers a tighter link between inflation and the relevant measures of economic slack once the persistence of real activity is no longer forced to reside entirely in the cycle.

A central implication of the framework is a rebalancing in the shocks that account for macroeconomic fluctuations. The U.S. sample features weak co-movement between inflation and real activity, together with episodes in which inflation shifts rapidly rather than through slow and persistent buildups. In the benchmark specification, flat Phillips curves and highly persistent cycles make it difficult to explain these inflation movements through cyclical channels without generating counterfactual movements in output and unemployment, leading the model to rely more heavily on cost-push shocks. By contrast, the scarring specification can explain a larger share of inflation dynamics through smaller and less persistent cyclical movements operating through steeper Phillips curves. At the same time, because these steeper slopes make inflation highly sensitive to the inflation-relevant cycle, the model cannot rely on cyclical innovations to explain most real-side business-cycle fluctuations. Instead, it shifts volatility toward the supply-driven stars and the endogenous scarring components of productive capacity.

These findings have important implications for the measurement of activity gaps and for monetary policy. In the scarring framework, the gap that enters the Phillips curve is the gap relative to productive or labor-market capacity, which includes the scars left by past cyclical conditions. The policy-relevant gap, however, is the deviation of output or unemployment from its purely supply-driven star. Scarring therefore separates the inflation-relevant gap from the monetary-policy-relevant gap. This distinction materially changes the historical interpretation of slack, especially around the GFC and the pre-pandemic expansion.

Finally, both the in-sample and out-of-sample evidence favor allowing for scarring. The

Bayesian model comparison indicates that the improvement in fit more than compensates for the additional parameters, and the pseudo out-of-sample forecasting exercise shows that the scarring specification improves forecasts of real activity and wage inflation while preserving comparable performance for price inflation. Taken together, these results suggest that relaxing the independence assumption between trends and cycles changes the inferred sources of macroeconomic fluctuations, the estimated strength of Phillips-curve relationships, and the measurement of the gaps that are central to monetary-policy analysis.

References

Alichi, Ali, Hayk Avetisyan, Douglas Laxton, Shalva Mkhatrishvili, Armen Nurbekyan, Lusine Torosyan, and Hou Wang. (2019) "Multivariate Filter Estimation of Potential Output for the United States: An Extension with Labor Market Hysteresis." IMF Working Paper WP/19/35, International Monetary Fund.

Aruoba, S. Borağan and Frank Schorfheide. (2011) "Sticky Prices versus Monetary Frictions: An Estimation of Policy Trade-Offs." *American Economic Journal: Macroeconomics*, 3, 60–90.

Assarsson, Bengt and Per Jansson. (1998) "Unemployment Persistence: The Case of Sweden." *Applied Economics Letters*, 5, 25–29.

Baqaee, David R., Emmanuel Farhi, and Kunal Sangani. (2024) "The Supply-Side Effects of Monetary Policy." *Journal of Political Economy*, 132, 1065–1112.

Basistha, Arabinda and Charles R. Nelson. (2007) "New measures of the output gap based on the forward-looking new Keynesian Phillips curve." *Journal of Monetary Economics, Elsevier*, 54, 498–511.

Bauer, Michael D. and Glenn D. Rudebusch. (2020) "Interest Rates under Falling Stars." *American Economic Review*, 110, 1316–54.

Bechný, Jakub. (2019) "Unemployment Hysteresis in the Czech Republic." *Prague Economic Papers*, 28, 532–546.

Benati, Luca and Thomas A. Lubik. (2022) "Searching for Hysteresis." FRB Richmond Working Paper No. 22-05.

Bianchi, Francesco, Giovanni Nicolò, and Dongho Song. (2023) "Inflation and Real Activity over the Business Cycle." Working Paper 31075, National Bureau of Economic Research.

Calvert Jump, Robert and Engelbert Stockhammer. (2023) "Revisiting the Hysteresis Hypothesis: An ARIMAX Approach." *Review of Keynesian Economics*, 11, 489–506.

Clark, Peter K. (1987) "The Cyclical Component of U. S. Economic Activity." *The Quarterly Journal of Economics*, 102, pp. 797–814.

Clark, Peter K. (1989) "Trend reversion in real output and unemployment." *Journal of Econometrics*, 40, 15 – 32.

Cogley, Timothy and Thomas Sargent. (2015) "Measuring Price-Level Uncertainty and Instability in the United States, 1850–2012." *The Review of Economics and Statistics*, 97, 827–838.

Del Negro, Marco, Marc Giannoni, and Frank Schorfheide. (2015) "Inflation in the Great Recession and New Keynesian Models." *American Economic Journal: Macroeconomics*, 7, 168–96.

Di Sanzo, Silvestro and Alicia Pérez-Alonso. (2011) "Unemployment and Hysteresis: A Nonlinear Unobserved Components Approach." *Studies in Nonlinear Dynamics & Econometrics*, 15, 1–29.

Diebold, Francis X and Roberto S Mariano. (1995) "Comparing Predictive Accuracy." *Journal of Business & Economic Statistics*, 13, 253–263.

Durbin, James and Siem Jan Koopman. (2002) "A simple and efficient simulation smoother for state space time series analysis." *Biometrika*, 89, 603–616.

Furlanetto, Francesco, Antoine Lepetit, Ørjan Robstad, Juan Rubio-Ramírez, and Pål Ulvedal. (2024) "Estimating Hysteresis Effects." *American Economic Journal: Macroeconomics*, forthcoming.

Galí, Jordi. (2022) "Insider-Outsider Labor Markets, Hysteresis, and Monetary Policy." *Journal of Money, Credit and Banking*, 54, 53–88.

Glick, Reuven, Sylvain Leduc, and Mollie Pepper. (2022) "Will Workers Demand Cost-of-Living Adjustments?" *FRBSF Economic Letter*, 2022, 1–6.

Gneiting, Tilmann and Adrian E Raftery. (2007) "Strictly proper scoring rules, prediction, and estimation." *Journal of the American statistical Association*, 102, 359–378.

González-Astudillo, Manuel and Jean-Philippe Laforte. (2025) "Estimates of the Natural Rate of Interest Consistent with a Supply-Side Structure and a Monetary Policy Rule for the US Economy." *International Journal of Central Banking*, 21, 137–199.

González-Astudillo, Manuel and John M Roberts. (2022) "When are trend–cycle decompositions of GDP reliable?" *Empirical Economics*, 62, 2417–2460.

Jaeger, Albert and Martin Parkinson. (1994) "Some Evidence on Hysteresis in Unemployment Rates." *European Economic Review*, 38, 329–342.

Jorda, Oscar, Sanjay R. Singh, and Alan M. Taylor. (2020) "The Long-Run Effects of Monetary Policy." NBER Working Paper No. 26666.

Kim, Sangjoon, Neil Shephard, and Siddhartha Chib. (1998) "Stochastic Volatility: Likelihood Inference and Comparison with ARCH Models." *The Review of Economic Studies*, 65, 361–393.

Kuttner, Kenneth N. (1994) "Estimating Potential Output as a Latent Variable." *Journal of Business & Economic Statistics*, 12, pp. 361–368.

Laubach, Thomas and John Williams. (2003) "Measuring the Natural Rate of Interest." *The Review of Economics and Statistics*, 85, 1063–1070.

Lepetit, Antoine. (2026) "Need for Speed: Scarring Effects and the Phillips Curve." Unpublished Manuscript.

Li, Mengheng and Ivan Mendieta-Muñoz. (2024) “Dynamic Hysteresis Effects.” *Journal of Economic Dynamics and Control*, 163, 104863.

Li, Mengheng and Ivan Mendieta-Muñoz. (2024) “Dynamic hysteresis effects.” *Journal of Economic Dynamics and Control*, 163, 104870.

Logeay, Camille and Silke Tober. (2006) “Hysteresis and the NAIRU in the Euro Area.” *Scottish Journal of Political Economy*, 53, 409–429.

Ma, Yueran and Karl Zimmermann. (2023) “Monetary Policy and Innovation.” Jackson Hole Symposium 2023.

Mertens, Elmar. (2016) “Measuring the Level and Uncertainty of Trend Inflation.” *The Review of Economics and Statistics*, 98, 950–967.

Morley, James C, Charles R Nelson, and Eric Zivot. (2003) “Why are the Beveridge-Nelson and unobserved-components decompositions of GDP so different?” *Review of Economics and Statistics*, 85, 235–243.

Mossfeldt, Marcus and Pär Österholm. (2011) “The Persistent Labour-Market Effects of the Financial Crisis.” *Applied Economics Letters*, 18, 637–642.

Queralto, Albert. (2022) “Monetary Policy in a Model of Growth.” International Finance Discussion Papers 1340. Washington: Board of Governors of the Federal Reserve System, https://doi.org/10.17016/IFDP.2022.1340.

Reifschneider, Dave, William Wascher, and David Wilcox. (2015) “Aggregate Supply in the United States: Recent Developments and Implications for the Conduct of Monetary Policy.” *IMF Economic Review*, 63, 71–109.

Stock, James H. and Mark Watson. (2007) “Why Has U.S. Inflation Become Harder to Forecast?” *Journal of Money, Credit and Banking*, 39, 3–33.

Verdinelli, Isabella and Larry Wasserman. (1991) “Bayesian analysis of outlier problems using the Gibbs sampler.” *Statistics and Computing*, 1, 105–117.

Watson, Mark W. (1986) “Univariate detrending methods with stochastic trends.” *Journal of Monetary Economics*, 18, 49 – 75.

Zaman, Saeed. (2025) “A unified framework to estimate macroeconomic stars.” *Review of Economics and Statistics*, 1–45.

Appendix

A Related Literature: Unobserved Components Models of Scarring and Hysteresis

This paper is related to a literature that uses unobserved components (UC) and state-space models to estimate whether cyclical fluctuations leave persistent or permanent effects on output, unemployment, or other measures of economic slack. The central issue in this literature is whether the trend component of real activity can be treated as independent of the cycle, as in standard trend-cycle decompositions, or whether past cyclical conditions feed back into the trend itself. In the latter case, shocks conventionally classified as demand or cyclical shocks can have persistent effects on the economy's productive capacity or on the natural rate of unemployment.

A first strand of this literature studies unemployment hysteresis. A classic contribution is Jaeger and Parkinson (1994), who propose a UC model in which unemployment is decomposed into a nonstationary natural-rate component and a stationary cyclical component. Hysteresis is modeled by allowing lagged cyclical unemployment to affect the current natural rate. This specification provides a direct empirical implementation of the idea that high unemployment can become partly self-perpetuating: a recession raises cyclical unemployment, and part of that cyclical increase is subsequently transmitted to the natural rate. Related papers extend this framework in several directions. Assarsson and Jansson (1998) apply a similar structure to Sweden, allowing for richer dynamics and additional output information. Logeay and Tober (2006) estimate hysteresis and NAIRU dynamics for the euro area, combining a UC decomposition of unemployment with a Phillips-curve equation. Di Sanzo and Pérez-Alonso (2011) allow the degree of hysteresis to vary nonlinearly across regimes, capturing the possibility that unemployment shocks have different effects on the natural rate depending on labor-market conditions. Mossfeldt and Österholm (2011) study the persistent labor-market effects of the financial crisis, while Bechný (2019) estimates unemployment hysteresis in a Bayesian UC framework. Taken together, these papers provide a long-running empirical tradition in which the natural rate of unemployment is no longer purely supply determined, but may itself respond to past cyclical slack.

A second strand of the literature applies similar ideas to potential output. In this class of models, hysteresis or scarring means that the output gap affects the path of potential output. Alichi et al. (2019) extend a multivariate filter for U.S. potential output to incorporate labor-market hysteresis. Their framework captures the idea that long and deep recessions can persistently damage labor-market performance and thereby reduce potential output, while sustained expansions can have the opposite effect. More closely related to our output block, Li and Mendieta-Muñoz (2024) introduce UC models in which the output gap affects potential output through a sequence of lagged hysteresis effects. Their framework is designed to separate long-run recession-induced effects from other trend-cycle interactions, and nests several existing UC specifications. This is an important contribution because it explicitly brings dynamic hysteresis into the UC estimation of potential output.

A third and especially relevant contribution is Calvert Jump and Stockhammer (2023).

Their starting point is the UC unemployment-hysteresis literature, but they show that the hysteresis coefficient can be identified from a reduced-form Phillips curve. In particular, they assume a law of motion for the natural rate,

$$n_t = \gamma n_{t-1} + \alpha u_{t-1},$$

and combine it with an accelerationist Phillips curve,

$$\Delta\pi_t = \beta(u_t - n_t) + v_t.$$

This delivers an ARIMAX representation in inflation and unemployment,

$$\Delta\pi_t = \gamma\Delta\pi_{t-1} + \beta u_t - \beta(\alpha + \gamma)u_{t-1} + v_t - \gamma v_{t-1}.$$

Writing the reduced-form coefficients as

$$\Delta\pi_t = \phi_1\Delta\pi_{t-1} + \phi_2 u_t + \phi_3 u_{t-1} + v_t + \phi_4 v_{t-1},$$

with the restriction $\phi_1 = -\phi_4$, the hysteresis coefficient can be recovered as

$$\alpha = -\frac{\phi_3}{\phi_2} - \phi_1.$$

This approach is important for our paper because it also uses Phillips-curve restrictions to discipline the measurement of hysteresis, rather than relying exclusively on the time-series decomposition of unemployment into trend and cycle. Their implementation, however, is focused on unemployment and price inflation, and it estimates a reduced-form ARIMAX equation that avoids specifying the high-frequency cyclical component of unemployment.

Our paper differs from this literature along four main dimensions. First, we derive the empirical specification from a structural New Keynesian model with history-dependent productive capacity. In that model, the Phillips curve depends on the gap between output and productive capacity, where productive capacity itself reflects both supply-driven potential and the scars left by past cyclical conditions. Equivalently, the Phillips curve can be written in terms of the level and change of the gap relative to the supply-driven trend. This structural restriction maps the coefficients on those terms into the degree of scarring or hysteresis.

Second, we jointly estimate scarring in both output and unemployment. On the output side, price inflation identifies the extent to which past output gaps affect productive capacity. On the unemployment side, wage inflation identifies the extent to which past unemployment gaps affect the labor-market trend. This joint treatment is important because output and unemployment are two central inputs into monetary-policy assessments of slack, and because wage inflation provides a natural source of discipline for labor-market scarring.

Third, we distinguish between two notions of trend. The first is the supply-driven star, which reflects slow-moving supply factors and corresponds to the object most closely related to the conventional policy concept of potential output or the natural rate. The second is productive capacity or the effective labor-market trend, which includes the endogenous effects of past cyclical conditions. Existing UC hysteresis models usually focus on whether the trend itself responds to the cycle. Our model separates the supply-driven star from the scarring component of the trend, which allows us to ask whether persistent movements in measured potential reflect supply disturbances or endogenous scars from past cyclical shocks.

Fourth, our identification problem is global and cross-equation. Output alone cannot cleanly distinguish a persistent cycle from endogenous movements in productive capacity: different combinations of cycle persistence, trend shocks, and scarring can generate the same reduced-form behavior of output. We therefore use price and wage Phillips curves to introduce additional cross-equation restrictions. The coefficients on the level and change of the output and unemployment gaps identify the degree of history dependence in productive and labor-market capacity. In this respect, the paper is closest in spirit to Calvert Jump and Stockhammer (2023), but it embeds the Phillips-curve identification idea in a multivariate UC framework disciplined by a structural NK model, extends it to output and wage inflation, and separates supply-driven stars from endogenous scarring components.

The paper is also related to the broader UC literature on output gaps and macroeconomic stars. The classic univariate output trend-cycle decompositions of Watson (1986) were extended to bivariate and multivariate settings by Clark (1989), Kuttner (1994), and subsequent work using inflation, unemployment, and other macroeconomic observables to discipline the estimation of latent trends. More recent large-scale multivariate UC frameworks estimate time-varying potential output, natural rates, and trend inflation using many indicators. In most of these models, however, trend and cycle are assumed to be independent objects or are allowed to comove without an explicit scarring interpretation. Our contribution is to incorporate a structural mechanism through which cyclical disturbances affect trend components, and to show how the resulting scarring parameters can be identified through price and wage dynamics.

B Identification of Model Parameters

Consider the following UC model for output:

$$\begin{aligned}
y_t &= y_t^* + w_t + \tilde{c}_t, \\
y_t^* &= \mu + y_{t-1}^* + \eta_t, \\
\tilde{c}_t &= \phi_1 \tilde{c}_{t-1} + \phi_2 \tilde{c}_{t-2} + \varepsilon_t, \\
w_t &= \rho w_{t-1} + \delta \tilde{c}_{t-1},
\end{aligned}$$

where w_t captures the hysteresis (or scarring) component. Here, $0 \leq \rho \leq 1$ and $\delta \geq 0$. If $\rho = \delta = 0$, there is no hysteresis; $\rho < 1$, $\delta > 0$ indicates scarring; and $\rho = 1$, $\delta > 0$ represents full hysteresis.

From an identification perspective, the structural parameter vector is

$$(\rho, \delta, \phi_1, \phi_2, \sigma_\eta^2, \sigma_\varepsilon^2),$$

and the reduced form will deliver a finite set of ARMA coefficients and autocovariances that can in principle be used to identify these parameters. The necessary order condition compares the dimension of these reduced-form objects with the number of structural unknowns, while the rank condition asks whether the resulting nonlinear mapping from structural parameters to reduced-form moments is injective.

B.1 Reduced-Form Representation for Output

For $\rho < 1$ and $\phi(L) = 1 - \phi_1 L - \phi_2 L^2$, the first difference of log GDP will be the following:

$$\Delta y_t = \mu + \eta_t + (1-L)(1-\rho L)^{-1}\delta L \phi(L)^{-1}\varepsilon_t + (1-L)\phi(L)^{-1}\varepsilon_t.$$

Or, rewritten, it will be the following:

$$\begin{aligned}(1-\rho L)\phi(L)\Delta y_t &= \mu(1-\rho)\phi(1) + (1-\rho L)\phi(L)\eta_t + (1-L)L\delta\varepsilon_t + (1-L)(1-\rho L)\varepsilon_t,\\ &= \mu(1-\rho)\phi(1) + (1-\rho L)\phi(L)\eta_t + \left[1-(\rho-\delta)L\right](1-L)\varepsilon_t.\end{aligned}$$

Now, because

$$\begin{aligned}(1-\rho L)(1-\phi_1 L - \phi_2 L^2) &= 1 - \phi_1 L - \phi_2 L^2 - \rho L + \rho\phi_1 L^2 + \rho\phi_2 L^3,\\ &= 1 - (\phi_1+\rho)L - (\phi_2 - \rho\phi_1)L^2 + \rho\phi_2 L^3\end{aligned}$$

and

$$\begin{aligned}\left[1-(\rho-\delta)L\right](1-L) &= 1 - L - (\rho-\delta)L + (\rho-\delta)L^2,\\ &= 1 - (1+\rho-\delta)L + (\rho-\delta)L^2,\end{aligned}$$

we have

$$(1-\rho L)\phi(L)\Delta y_t = \mu(1-\rho)\phi(1) + \eta_t - (\phi_1+\rho)\eta_{t-1} - (\phi_2-\rho\phi_1)\eta_{t-2} + \rho\phi_2\eta_{t-3} + \varepsilon_t - (1+\rho-\delta)\varepsilon_{t-1} + (\rho-\delta)\varepsilon_{t-2}.$$

This implies an ARMA(3,3) representation for Δy_t. The corresponding reduced form for y_t is ARIMA(3,1,3), with three reduced-form AR coefficients and three reduced-form MA coefficients. Together with second moments, there are as many reduced-form restrictions as structural parameters $(\rho, \delta, \phi_1, \phi_2, \sigma_\eta^2, \sigma_\varepsilon^2)$, so the *necessary order condition* for identification is satisfied in this case.

The autocovariance function of the right-hand side is given by

$$\begin{aligned}\gamma_0 &= \sigma_\eta^2[1 + (\phi_1+\rho)^2 + (\phi_2-\rho\phi_1)^2 + \rho^2\phi_2^2] + \sigma_\varepsilon^2[1 + (1+\rho-\delta)^2 + (\rho-\delta)^2],\\ \gamma_1 &= [-(\phi_1+\rho) + (\phi_2-\rho\phi_1)(\phi_1+\rho) - \rho\phi_2(\phi_2-\rho\phi_1)]\sigma_\eta^2\\ &\quad - [(1+\rho-\delta) + (\rho-\delta)(1-\rho-\delta)]\sigma_\varepsilon^2,\\ \gamma_2 &= -[(\phi_2-\rho\phi_1) + \rho\phi_2(\phi_1+\rho)]\sigma_\eta^2 + (\rho-\delta)\sigma_\varepsilon^2,\\ \gamma_3 &= \rho\phi_2\sigma_\eta^2.\end{aligned}$$

This can be written compactly as

$$\begin{bmatrix}\gamma_0\\ \gamma_1\\ \gamma_2\\ \gamma_3\end{bmatrix} = \begin{bmatrix} 1+(\phi_1+\rho)^2+(\phi_2-\rho\phi_1)^2+\rho^2\phi_2^2 & 1+(1+\rho-\delta)^2+(\rho-\delta)^2 \\ -(\phi_1+\rho)+(\phi_2-\rho\phi_1)(\phi_1+\rho)-\rho\phi_2(\phi_2-\rho\phi_1) & -[(1+\rho-\delta)+(\rho-\delta)(1-\rho-\delta)] \\ -[(\phi_2-\rho\phi_1)+\rho\phi_2(\phi_1+\rho)] & \rho-\delta \\ \rho\phi_2 & 0 \end{bmatrix} \begin{bmatrix}\sigma_\eta^2\\ \sigma_\varepsilon^2\end{bmatrix}.$$

Conditional on $(\rho, \delta, \phi_1, \phi_2)$, the upper 2×2 block of the matrix in the last expression typically has full rank, so $(\sigma_\eta^2, \sigma_\varepsilon^2)$ are identified given the other parameters. However, at the level of $(\rho, \delta, \phi_1, \phi_2)$ themselves the *rank condition* fails. The autoregressive coefficients depend on (ϕ_1, ϕ_2, ρ) through $(\phi_1 + \rho, \phi_2 - \rho\phi_1, \rho\phi_2)$, while the moving-average coefficients depend on (ρ, δ) through the combinations $(1 + \rho - \delta)$ and $(\rho - \delta)$. As shown next, this structure implies that different values of $(\rho, \delta, \phi_1, \phi_2)$ can generate identical reduced-form AR and MA coefficients, so the mapping from structural parameters to reduced-form moments is not one-to-one even though the order condition is satisfied.

B.2 Ambiguity in (ϕ_1, ϕ_2, ρ)

The autoregressive portion of the reduced form (the left-hand side term, $(1-\rho L)\phi(L)\Delta y_t$) is characterized by coefficients

$$\tilde{\phi}_1 \equiv \phi_1 + \rho, \qquad \tilde{\phi}_2 \equiv \phi_2 - \rho\phi_1, \qquad \tilde{\phi}_3 \equiv \rho\phi_2.$$

The mapping from $(\tilde{\phi}_1, \tilde{\phi}_2, \tilde{\phi}_3)$ to (ϕ_1, ϕ_2, ρ) is governed by the cubic equation

$$\rho^3 - \tilde{\phi}_1\rho^2 - \tilde{\phi}_2\rho + \tilde{\phi}_3 = 0.$$

Because cubic equations generally have multiple real roots, (ϕ_1, ϕ_2, ρ) cannot be uniquely recovered from $(\tilde{\phi}_1, \tilde{\phi}_2, \tilde{\phi}_3)$. In terms of identification, this means that the Jacobian from (ϕ_1, ϕ_2, ρ) to $(\tilde{\phi}_1, \tilde{\phi}_2, \tilde{\phi}_3)$ is not globally invertible: the rank condition for unique recovery of (ϕ_1, ϕ_2, ρ) fails despite the fact that the order condition is satisfied. This implies that even if we imposed a restriction such as $\rho = \delta$, we would not achieve unique identification of the hysteresis parameters from the output-only reduced form.

B.2.1 Case $\rho = 1$ (hysteresis): ARMA(2,2) Representation

When $\rho = 1$, the model simplifies to

$$\phi(L)\Delta y_t = \mu\phi(1) + \phi(L)\eta_t + [1 + (\delta - 1)L]\varepsilon_t,$$

which is an ARMA(2,2) process. In this case, the relevant structural parameters on the MA side are $(\delta, \sigma_\eta^2, \sigma_\varepsilon^2)$ and the reduced-form information from the MA side is contained in three autocovariances $(\gamma_0, \gamma_1, \gamma_2)$. Thus the *order condition* for identifying $(\delta, \sigma_\eta^2, \sigma_\varepsilon^2)$ using these moments is satisfied: the number of moments equals the number of unknowns.

The MA autocovariance structure is

$$\begin{bmatrix}\gamma_0\\ \gamma_1\\ \gamma_2\end{bmatrix} = \begin{bmatrix}1+\phi_1^2+\phi_2^2 & 1+(1-\delta)^2\\ -\phi_1(1-\phi_2) & -(1-\delta)\\ -\phi_2 & 0\end{bmatrix}\begin{bmatrix}\sigma_\eta^2\\ \sigma_\varepsilon^2\end{bmatrix}.$$

Solving backwards, σ_η^2 is pinned down from γ_2, and (γ_0, γ_1) then determine $(1-\delta)$ and σ_ε^2 through a nonlinear system. Even in this simpler case, however, δ enters quadratically through terms involving $(1-\delta)^2$, which generically leads to two admissible solutions for $(\delta, \sigma_\varepsilon^2)$ that generate the same $(\gamma_0, \gamma_1, \gamma_2)$. In other words, the local rank condition can hold at each solution, but global uniqueness fails: the mapping from $(\delta, \sigma_\eta^2, \sigma_\varepsilon^2)$ to the MA autocovariances is two-to-one. Thus, the model remains underidentified when only output is observed. This finding is shown in Li and Mendieta-Muñoz (2024).

An extreme way to recover uniqueness would be to impose $\delta = 1$ *a priori*. This eliminates the quadratic term and collapses the parameter space so that $(\sigma_\eta^2, \sigma_\varepsilon^2)$ can be uniquely recovered from the autocovariances. However, this is an identifying restriction imposed by assumption rather than by the data; it enforces identification by severely restricting the admissible set of hysteresis mechanisms and is therefore too restrictive from an economic point of view.

B.3 Will Adding an Inflation Block Allow for Identification?

The inflation block is defined as:

$$\begin{aligned}\pi_t &= \pi_t^* + \kappa\tilde{c}_t, \quad \kappa \geq 0,\\ \pi_t^* &= \pi_{t-1}^* + \eta_t^{\pi^*},\end{aligned}$$

with shocks satisfying

$$\operatorname{var}(\eta_t^{\pi^*}) = \sigma^2_{\eta^{\pi^*}},$$

and all shocks are mutually orthogonal.

Then, the change in the inflation rate will be

$$\Delta\pi_t = \eta_t^{\pi^*} + \kappa(1-L)\phi(L)^{-1}\varepsilon_t,$$

which can be written as follows:

$$\begin{aligned}\phi(L)\Delta\pi_t &= \phi(L)\eta_t^{\pi^*} + \kappa(1-L)\varepsilon_t\\ &= \eta_t^{\pi^*} - \phi_1\eta_{t-1}^{\pi^*} - \phi_2\eta_{t-2}^{\pi^*} + \kappa\varepsilon_t - \kappa\varepsilon_{t-1}.\end{aligned}$$

This implies the inflation rate is an ARMA(2,2) process with the AR component being the same as that of the cycle. The MA portion has the following autocovariance function:

$$\begin{aligned}\gamma_0^\pi &= (1+\phi_1^2+\phi_2^2)\sigma^2_{\eta_t^{\pi^*}} + 2\kappa^2\sigma_\varepsilon^2,\\ \gamma_1^\pi &= -\phi_1(1-\phi_2)\sigma^2_{\eta_t^{\pi^*}} - \kappa^2\sigma_\varepsilon^2,\end{aligned}$$

$$\gamma_2^{\pi} = -\phi_2 \sigma^2_{\eta_t^{\pi^*}}.$$

We could get additional reduced-form restrictions from the covariance between Δy_t and $\Delta \pi_t$:

$$\gamma_0^{y,\pi} = \sigma_\varepsilon^2 \kappa(2 + \rho - \delta).$$

Adding inflation therefore increases the number of observable moments relative to the baseline output-only model, so at the level of a simple counting argument (order condition) identification becomes *feasible*: there are now more moments than structural parameters.

However, these extra moments do not break the functional dependence that caused the rank condition to fail in the output-only case. Inflation depends solely on the cycle, and the reduced-form dynamics of $\Delta\pi_t$ involve ε_t only through the same combinations that appear in the output block. As a result, under general values of ρ and δ, multiple combinations of $(\rho, \delta, \sigma_\eta^2, \sigma_\varepsilon^2, \sigma^2_{\eta^{\pi^*}}, \kappa)$ still generate the same joint autocovariance structure for $(\Delta y_t, \Delta \pi_t)$. Under $\rho = \delta \neq 0$, there remains the problem of obtaining ρ uniquely, and if $\rho = 1$ and $\delta > 0$, we still have non uniqueness in δ, as indicated above. In short, while the inflation block adds more equations, it does not alter the fact that the mapping from the hysteresis parameters to reduced-form moments is not one-to-one: the rank condition continues to fail, and the lack of identification persists.

B.4 When does an Inflation Equation allow for Identification?

Now consider an inflation equation consistent with scarring/hysteresis dynamics:

$$\begin{aligned}
\pi_t &= \pi_t^* + \kappa_1(y_t - y_t^*) + \kappa_2 \Delta(y_t - y_t^*) + \varepsilon_t^{\pi}, \\
\pi_t^* &= \pi_{t-1}^* + \eta_t^{\pi^*},
\end{aligned}$$

where $\kappa_1, \kappa_2 \geq 0$ but both cannot be zero at the same time. The introduction of the error term ε_t^{π} does not change the structure of the identification problem: it simply adds measurement noise.

This inflation equation can be rewritten as

$$\pi_t = \pi_t^* + \kappa(y_t - \tilde{y}_t^*) + \varepsilon_t^{\pi}, \qquad \kappa = \kappa_1 + \kappa_2,$$

where

$$\tilde{y}_t^* = y_t^* + \frac{\kappa_2}{\kappa}(y_{t-1} - y_{t-1}^*).$$

Defining $w_t = \tilde{y}_t^* - y_t^*$ yields

$$w_t = \frac{\kappa_2}{\kappa} w_{t-1} + \frac{\kappa_2}{\kappa}(y_{t-1} - \tilde{y}_{t-1}^*),$$

which has the same structure as the hysteresis process for output,

$$w_t = \rho w_{t-1} + \delta \tilde{c}_{t-1}, \qquad \text{with } \rho = \delta = \frac{\kappa_2}{\kappa_1 + \kappa_2}.$$

Notice that $\kappa_1 = 0$ implies full hysteresis whereas $\kappa_2 = 0$ implies lack of scarring or hysteresis.

The inclusion of this richer inflation equation introduces a new set of observable cross-equation covariances linking (π_t, y_t) that are not redundant with those already implied by the output block. In particular, the Phillips curve coefficients (κ_1, κ_2) can be identified statistically as the regression coefficients of $(\pi_t - \pi_t^*)$ on $(y_t - y_t^*, \Delta y_t - \Delta y_t^*)$:

$$(\kappa_1, \kappa_2)' = [\mathrm{Var}(\mathrm{gap}_t, \Delta \mathrm{gap}_t)]^{-1} \, \mathrm{Cov}((\mathrm{gap}_t, \Delta \mathrm{gap}_t), \pi_t - \pi_t^*), \qquad \mathrm{gap}_t = y_t - y_t^*.$$

As long as $\mathrm{Var}(\mathrm{gap}_t, \Delta \mathrm{gap}_t)$ is nonsingular and ε_t^π is orthogonal to $(\mathrm{gap}_t, \Delta \mathrm{gap}_t)$, (κ_1, κ_2) are uniquely identified. In terms of identification, this means that both the order and rank conditions are now satisfied for (κ_1, κ_2): there are enough independent cross-equation moments, and the covariance matrix of regressors is invertible.

Consequently,

$$\rho = \delta = \frac{\kappa_2}{\kappa_1 + \kappa_2}$$

is also uniquely identified. This cross-equation restriction eliminates the multiplicity of solutions present in the output-only UC model by tying the hysteresis mechanism directly to observable inflation-output comovements.

Once (ρ, δ) are identified, the remaining parameters $(\phi_1, \phi_2, \sigma_\eta^2, \sigma_\varepsilon^2)$ can be recovered uniquely from the reduced-form equations of Δy_t. At this point, both the necessary order condition and the rank condition for the full parameter vector are satisfied: the mapping from the structural parameters $(\rho, \delta, \phi_1, \phi_2, \sigma_\eta^2, \sigma_\varepsilon^2)$ to the reduced-form moments of (y_t, π_t) becomes one-to-one.

B.5 Simulation Exercise

To confirm the model's parameters are identified, we perform a Monte Carlo experiment in which we simulate and estimate the following model 1,000 times by maximum likelihood:

$$\begin{aligned}
y_t &= \tilde{y}_t + \tilde{c}_t, \\
\tilde{y}_t &= y_t^* + w_t^y, \\
y_t^* &= \mu + y_{t-1}^* + \eta_t^{y^*}, \qquad \eta_t^{y^*} \sim \text{i.i.d.} N(0, 0.4^2), \qquad \mu = 0.5, y_0^* = 0, \\
\tilde{c}_t &= 1.5\tilde{c}_{t-1} - 0.6\tilde{c}_{t-2} + \varepsilon_t, \qquad \varepsilon_t \sim \text{i.i.d.} N(0, 0.6^2), \quad \tilde{c}_{t-1} = \tilde{c}_{t-2} = 0 \\
\pi_t &= \pi_t^* + (\kappa_1 + \kappa_2)\tilde{c}_t + \varepsilon_t^\pi, \qquad \varepsilon_t^\pi \sim \text{i.i.d.} N(0, 0.6^2), \quad \kappa_1 = 0.05, \kappa_2 = 0.35, \\
\pi_t^* &= \pi_{t-1}^* + \eta_t^{\pi^*}, \qquad \eta_t^{\pi^*} \sim \text{i.i.d.} N(0, 0.1^2), \qquad \pi_0^* = 2, \\
w_t^y &= \rho^y w_{t-1}^y + \delta^y \tilde{c}_{t-1}, \qquad \rho^y = \delta^y = \frac{\kappa_2}{\kappa_1 + \kappa_2}, \quad w_0^y = 0, \\
u_t &= \tilde{u}_t - 0.25\tilde{c}_t - 0.25\tilde{c}_{t-1} + \upsilon_t, \qquad \upsilon_t \sim \text{i.i.d.} N(0, 0.05^2), \\
\tilde{u}_t &= u_t^* + w_t^u, \\
u_t^* &= u_{t-1}^* + \eta_t^{u^*}, \qquad \eta_t^{u^*} \sim \text{i.i.d.} N(0, 0.1^2), \qquad u_0^* = 4, \\
\pi_t^w &= 2 + \pi_t^* + (\gamma_1 + \gamma_2)(u_t - \tilde{u}_t) + \varepsilon_t^{\pi^w}, \qquad \varepsilon_t^{\pi^w} \sim \text{i.i.d.} N(0, 0.5^2), \quad \gamma_1 = -0.2, \gamma_2 = -0.30,
\end{aligned}$$

Figure B.1: Distribution of model parameters estimates (part 1)

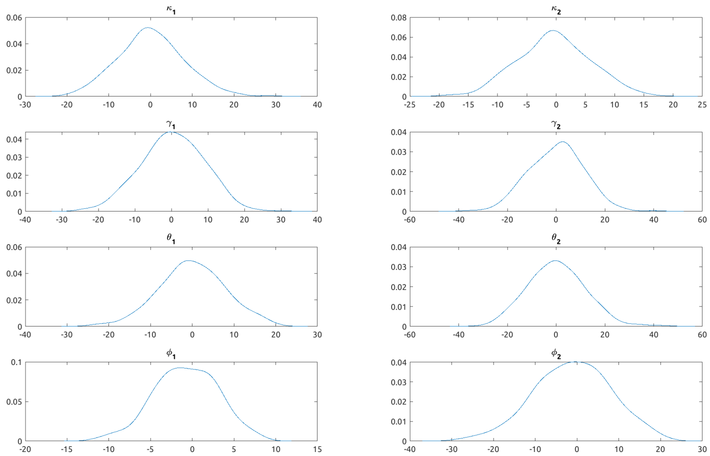

Note: The graphs show the distribution of the percent deviation of the estimator from the true parameter value.

$$w_t^u = \rho^u w_{t-1}^u + \delta^u (u_{t-1} - \tilde{u}_{t-1}), \qquad \rho^u = \delta^u = \frac{\gamma_2}{\gamma_1 + \gamma_2}, \quad w_0^u = 0.$$

The distributions of estimates appears in figures B.1 and B.2. As can be seen, the estimates are well behaved, centered around the true values of the parameters and with well behaved distributions, confirming our setup is able to identify all the parameters of the model with scarring.

Figure B.2: Distribution of model parameters estimates (part 2)

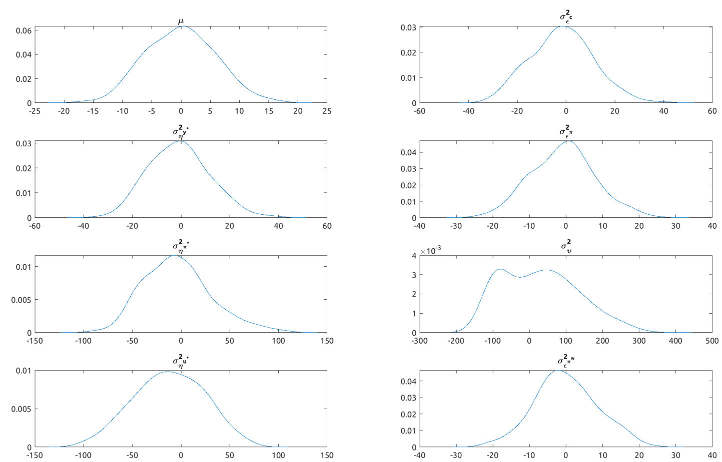

Note: The graphs show the distribution of the estimator minus the true parameter value.

Figure C.1: Outliers

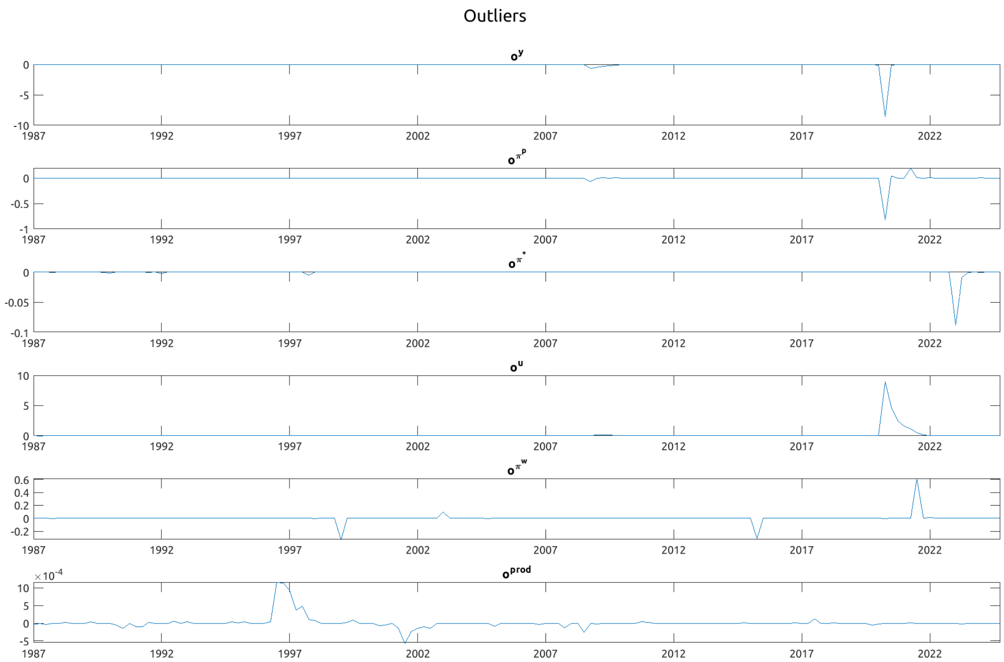

C Outliers Estimates

This section shows the estimated outliers of the model with scarring as well as their estimated probabilities in Figures C.1 and C.2, respectively. The only significant outliers in our sample, from a probabilistic point of view (probabilities close or equal to one), occur in GDP and the unemployment rate during the COVID-19 pandemic, more precisely in 2020:Q2 for both GDP and the unemployment rate, and 2020:Q3 for the unemployment rate.

Figure C.2: Probability of Outliers

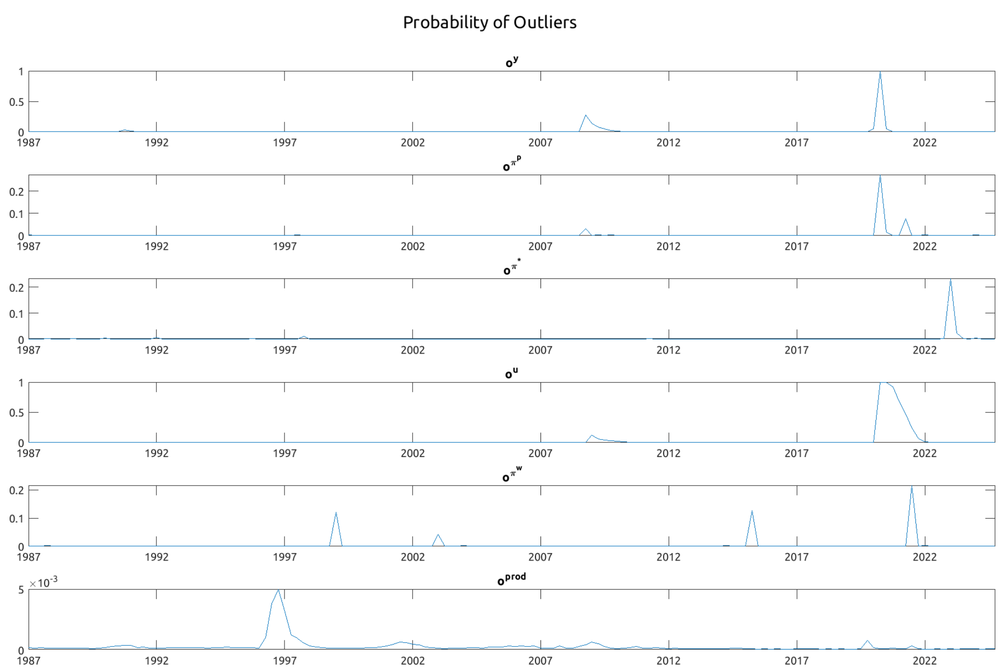

D Shock Decomposition and Additional Figures

Figure D.1: GDP Shock Decomposition

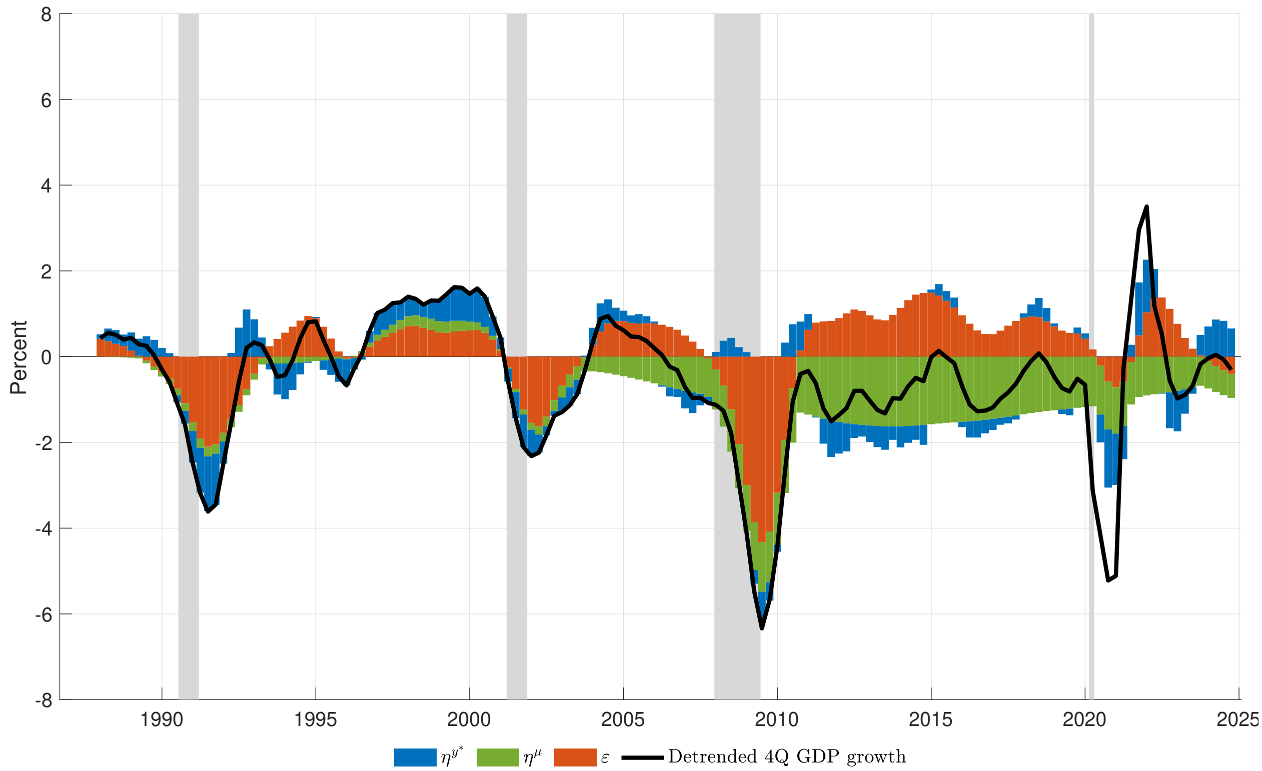

(a) Benchmark

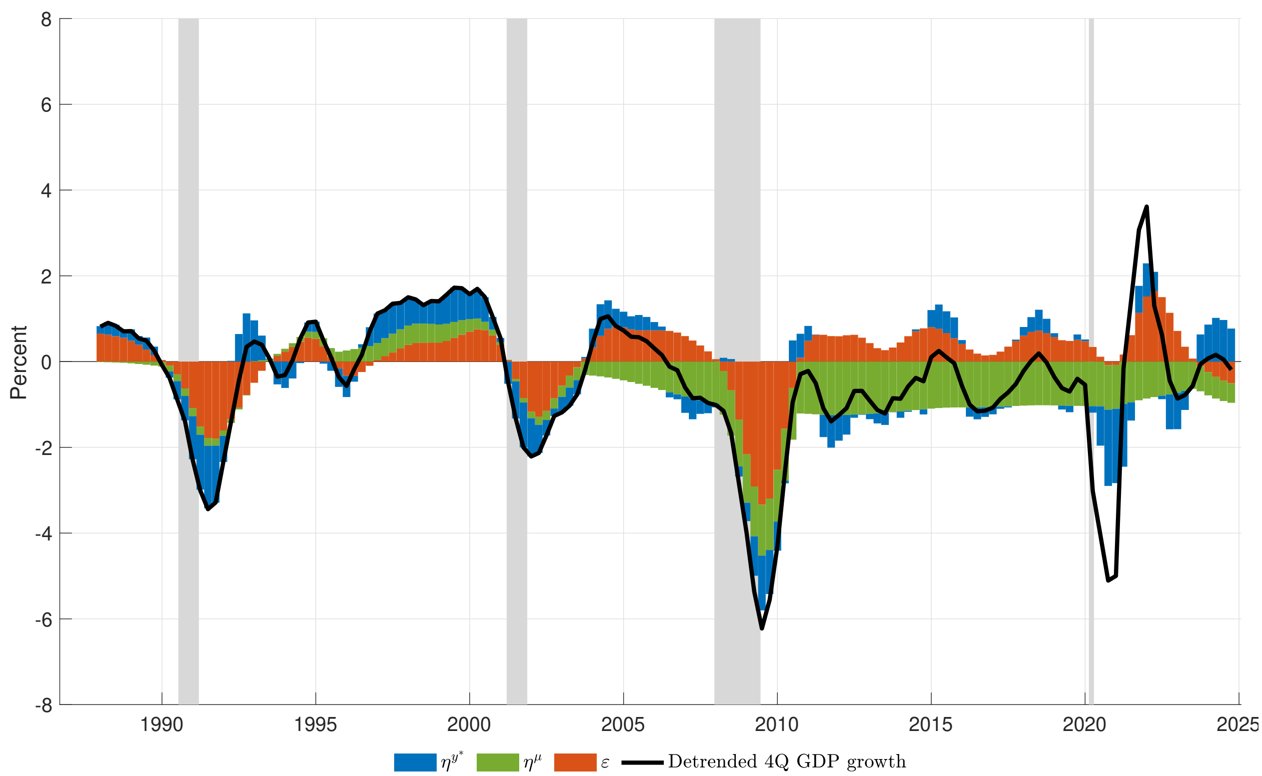

(b) Scarring

Note: Shock decompositions obtained at the posterior mean estimates. The four-quarter growth rate of the GDP data is detrended by removing the contribution from the initial conditions. Difference between the black line and the sum of the contribution shown in these figures correspond to the contribution from the outlier process.

Figure D.2: Unemployment Shock Decomposition

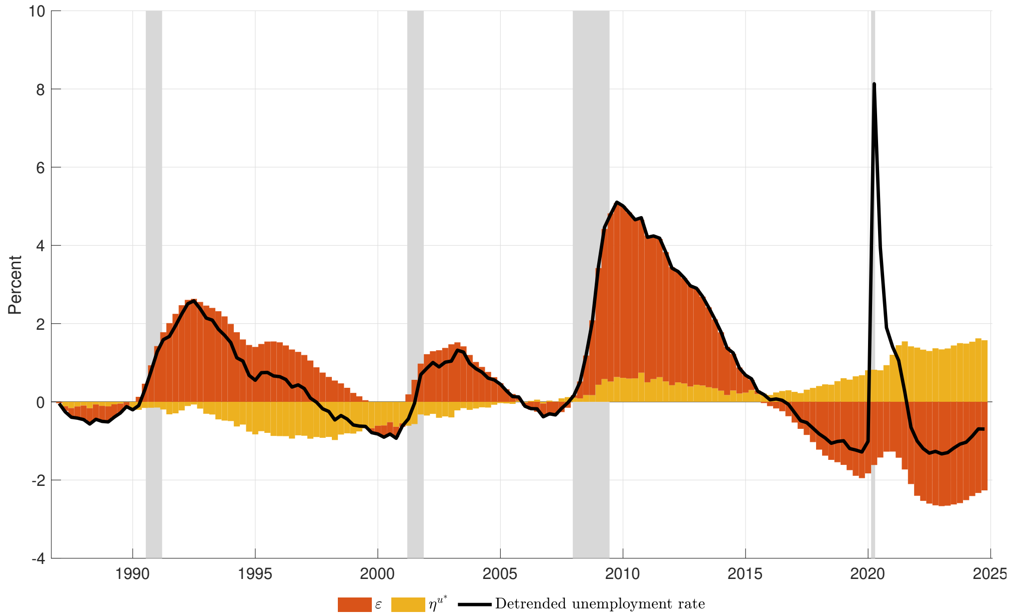

(a) Benchmark

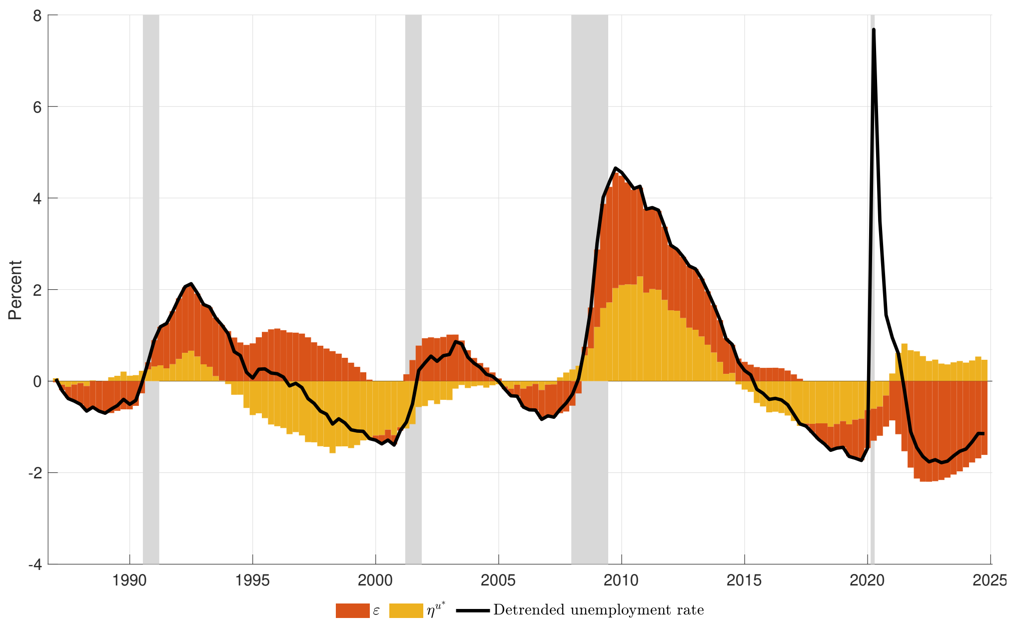

(b) Scarring

Note: Shock decompositions obtained at the posterior mean estimates. The unemployment rate data is detrended by removing the contribution from the initial conditions. Difference between the black line and the sum of the contribution shown in these figures correspond to the contribution from the outlier process.

Figure D.3: Inflation and Expected Inflation

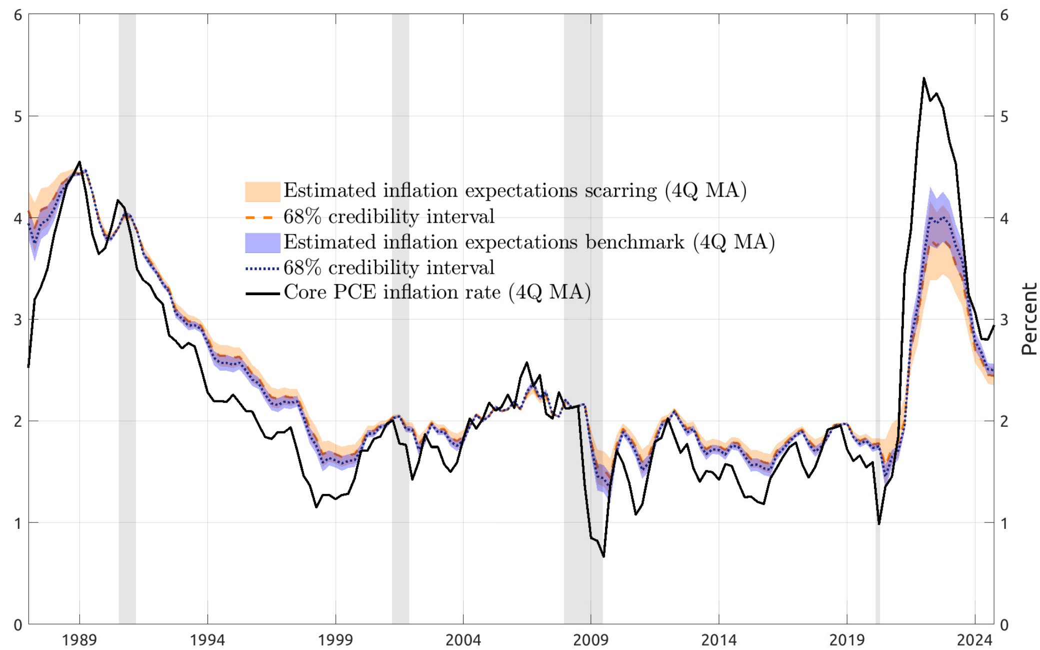

Figure D.4: Wage Inflation Shock Decomposition

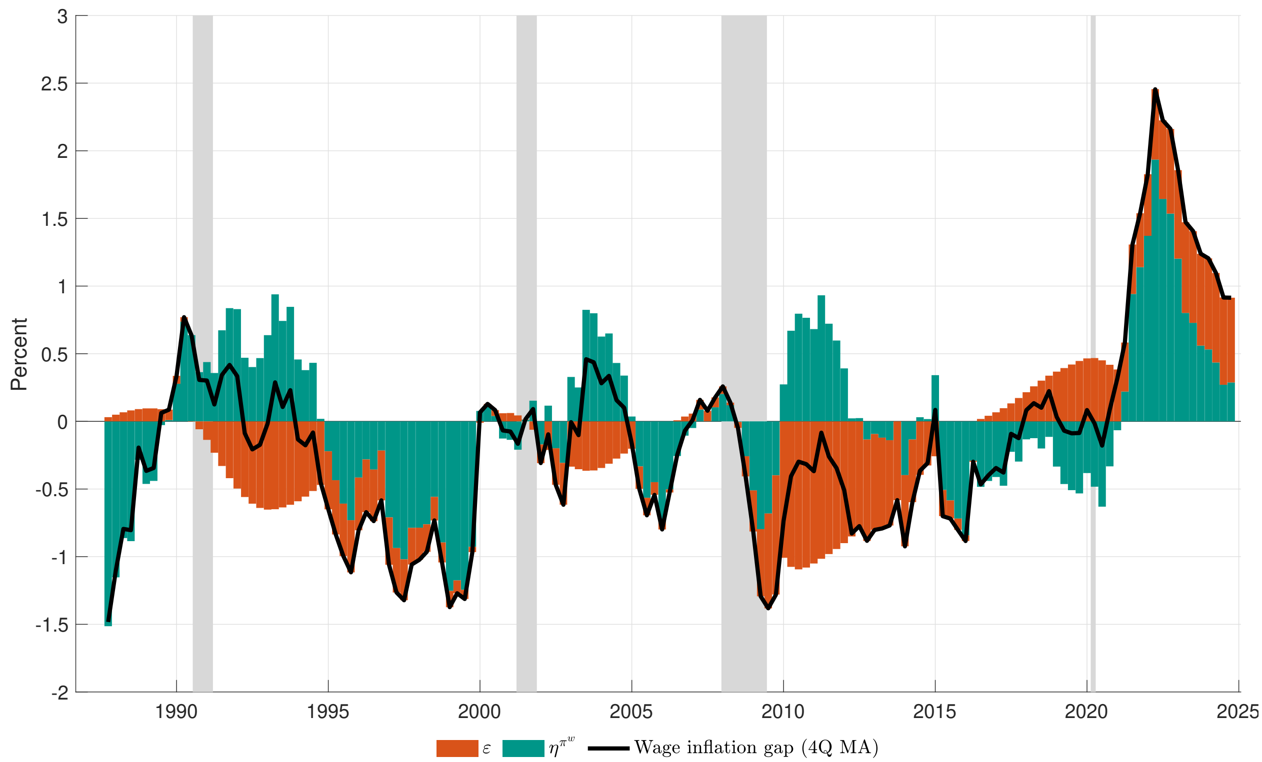

(a) Benchmark

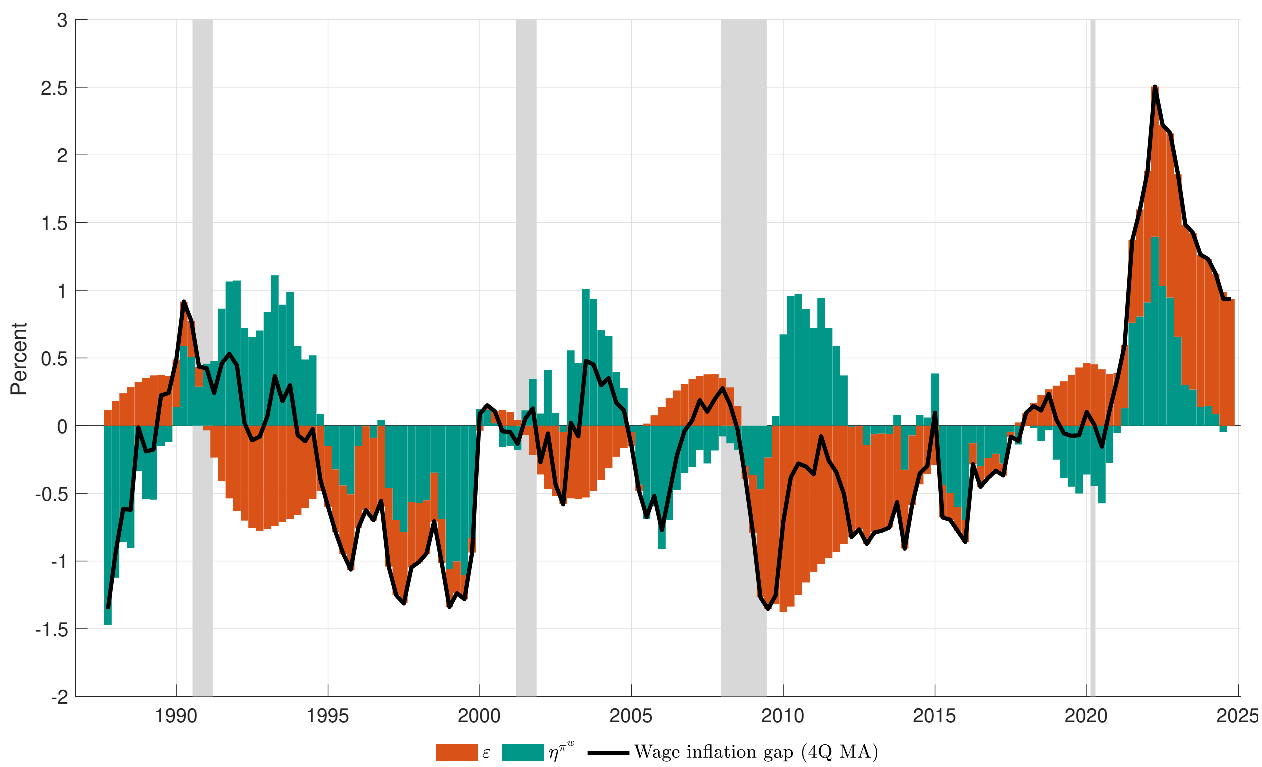

(b) Scarring

Note: Shock decompositions obtained at the posterior mean estimates. The black line corresponds to the difference between the wage inflation data and the sum of the contributions from the state of the Kalman filter's initial conditions, the trend inflation process and the trend productivity growth rate.

E A Model with Hysteresis

This appendix considers the limiting case of the UC model with scarring in which cyclical disturbances have permanent effects on productive capacity. This corresponds to the hysteresis case discussed in Section 3.

E.1 Specification

Recall that productive capacity is defined as

$$\tilde{y}_t^* = y_t^* + w_t^y, \tag{E.1}$$

where y_t^* is the purely supply-driven output trend and w_t^y captures the cumulative effects of past cyclical deviations.

From equation (11) in the main text, the scarring component evolves as

$$w_t^y = \delta^y \left(y_{t-1} - y_{t-1}^*\right). \tag{E.2}$$

Imposing hysteresis corresponds to setting $\kappa_1 = 0$, which implies

$$\delta^y = \frac{\kappa_2}{\kappa_1 + \kappa_2} = 1.$$

Under this restriction,

$$w_t^y = w_{t-1}^y + \tilde{c}_{t-1}, \tag{E.3}$$

or equivalently,

$$\Delta w_t^y = \tilde{c}_{t-1}. \tag{E.4}$$

Thus, w_t^y follows a unit-root process driven by lagged cyclical conditions. Deviations of productive capacity $\tilde{y}_t^*$ from the supply-driven trend y_t^* are therefore permanent. In terms of the autoregressive representation discussed in the main text, this corresponds to

$$\rho^y = 1.$$

The Phillips curve simplifies to

$$\pi_t = \beta\pi_{t-1} + (1-\beta)\pi_t^* + \kappa_2\Delta(y_t - y_t^*) + \varepsilon_t^\pi, \tag{E.5}$$

so that only changes in the output gap affect inflation dynamics, consistent with the hysteresis case derived in Section 2.

E.2 Results

Table E.1 reports posterior estimates for the hysteresis specification. Relative to scarring, both the price and wage Phillips curves are steeper (recall that we keep our assumption of scarring in the labor market). Moreover, the persistence/sensitivity of the scarring mechanism in the unemployment rate, given by the coefficient $\rho^u = \delta^u$, is lower in the hysteresis specification, indicating that unemployment scarring is less pronounced once output is allowed to experience hysteresis.

Table E.1: Prior Distributions and Estimation Results

		Benchmark		Scarring		Hysteresis	
	Prior Dist.	Post. Mean	68% CI	Post. Mean	68% CI	Post. Mean	68% CI
ϕ_1	N(1.5,1)	1.74	[1.67,1.81]	1.25	[1.02,1.48]	0.73	[0.41,1.03]
ϕ_2	N(-0.6,1)	−0.75	[-0.83,-0.68]	−0.30	[-0.52,-0.09]	0.17	[-0.13,0.49]
θ_1	N(-0.35,0.25)	−0.30	[-0.43,-0.17]	−0.35	[-0.51,-0.19]	−0.49	[-0.68,-0.28]
θ_2	N(-0.20,0.25)	−0.42	[-0.53,-0.30]	−0.47	[-0.61,-0.33]	−0.55	[-0.73,-0.37]
β	N(0.7,0.5)	0.57	[0.49,0.66]	0.49	[0.38,0.61]	0.45	[0.33,0.57]
κ_1	N(0.1,0.5)	0.09	[0.06,0.12]	0.19	[0.08,0.31]	0	—
κ_2	N(0,0.5)	0	—	0.28	[0.10,0.46]	1.01	[0.64,1.37]
λ	N(-0.2,1)	−0.59	[-0.72,-0.46]	−0.65	[-0.79,-0.52]	−0.68	[-0.83,-0.53]
β^w	N(0.8,0.5)	0.40	[0.31,0.49]	0.34	[0.23,0.46]	0.29	[0.18,0.40]
γ_1	N(-0.1,0.5)	−0.15	[-0.21,-0.10]	−0.36	[-0.61,-0.14]	−0.94	[-1.33,-0.54]
γ_2	N(0,0.5)	0	—	−0.31	[-0.53,-0.09]	−0.29	[-0.52,-0.07]
y_0^*	N(911.9,5)	911.9	[910.9,913.3]	911.9	[910.5,913.5]	911.9	[907.0,916.7]
μ_0	N(1,1)	0.76	[0.62,0.89]	0.74	[0.61,0.88]	1.05	[0.88,1.22]
π_0^*	N(5,2)	4.88	[4.74,5.02]	4.88	[4.74,5.03]	4.88	[4.74,5.03]
u_0^*	N(5.9,2)	4.87	[4.09,5.60]	5.22	[4.50,5.93]	5.91	[5.51,6.34]
g_0^*	N(1.8,1)	1.77	[1.70,1.84]	1.77	[1.70,1.84]	1.77	[1.70,1.84]
κ		0.09	[0.06,0.12]	0.48	[0.23,0.71]	1.01	[0.64, 1.37]
γ		−0.15	[-0.21,-0.10]	−0.67	[-0.99,-0.32]	−1.24	[-1.69, -0.76]
$\rho^y = \delta^y$		0	—	0.58	[0.35,0.79]	1	—
$\rho^u = \delta^u$		0	—	0.47	[0.21,0.71]	0.24	[0.07, 0.40]

Note: “N” stands for normal distribution. The first parameter is the mean and the second is the standard deviation.

Figure E.1: Stochastic Volatility Estimates

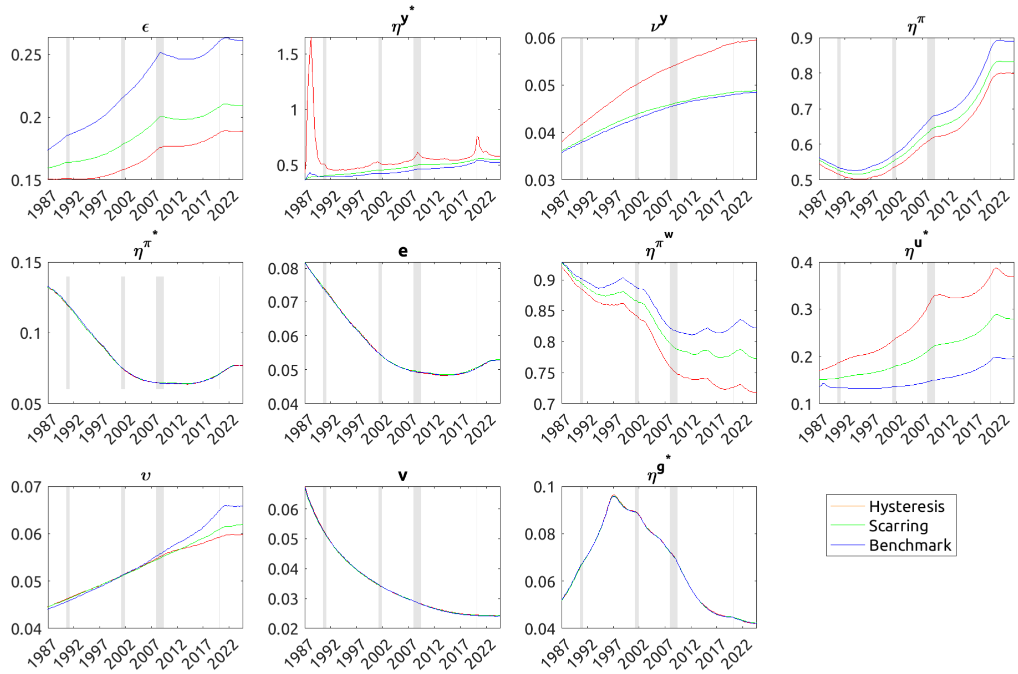

A second feature the hysteresis specification delivers that is distinct from scarring can be seen in Figure E.1 which shows the estimated stochastic volatility of the shocks (red lines correspond to hysteresis). First, under hysteresis, the cycle experience much less volatile shocks. Second, purely supply-driven shocks have larger variances under this specification. Third, The hysteresis specification relies less on cost-push shocks than the scarring's.

As a consequence, the estimated cycle $\tilde{c}_t$ under hysteresis (the yellow line in Figure E.3) is much shallower than under scarring which means $\tilde{y}_t$ will vary more at business cycle frequencies than the scarring specification, as shown in Figure E.2. Finally, trend unemployment ($\tilde{u}_t$) estimates do not appear to differ significantly between the scarring and hysteresis specifications, as shown in Figure E.4.

Figure E.2: Productive Capacity with History Dependence

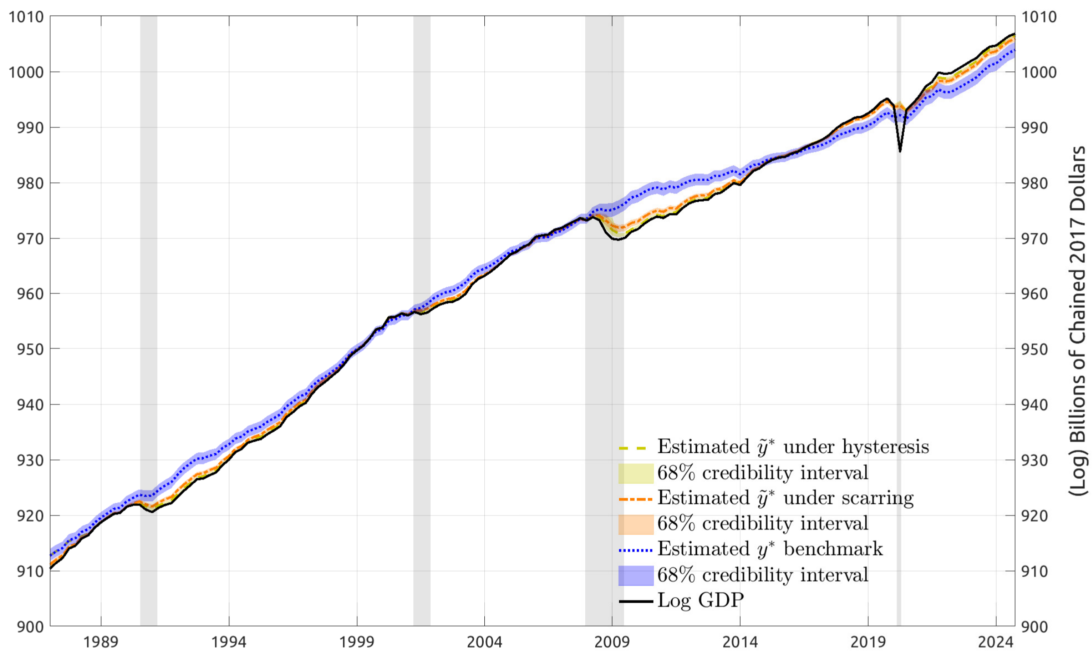

Figure E.3: Output Gap with History Dependence

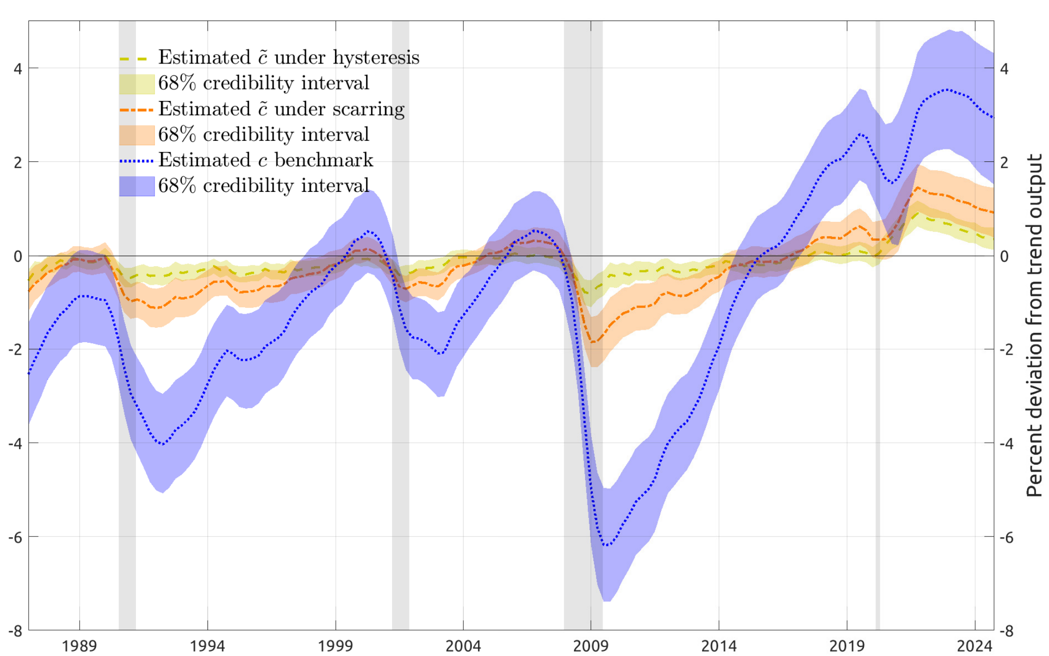

Figure E.4: Trend Unemployment with History Dependence

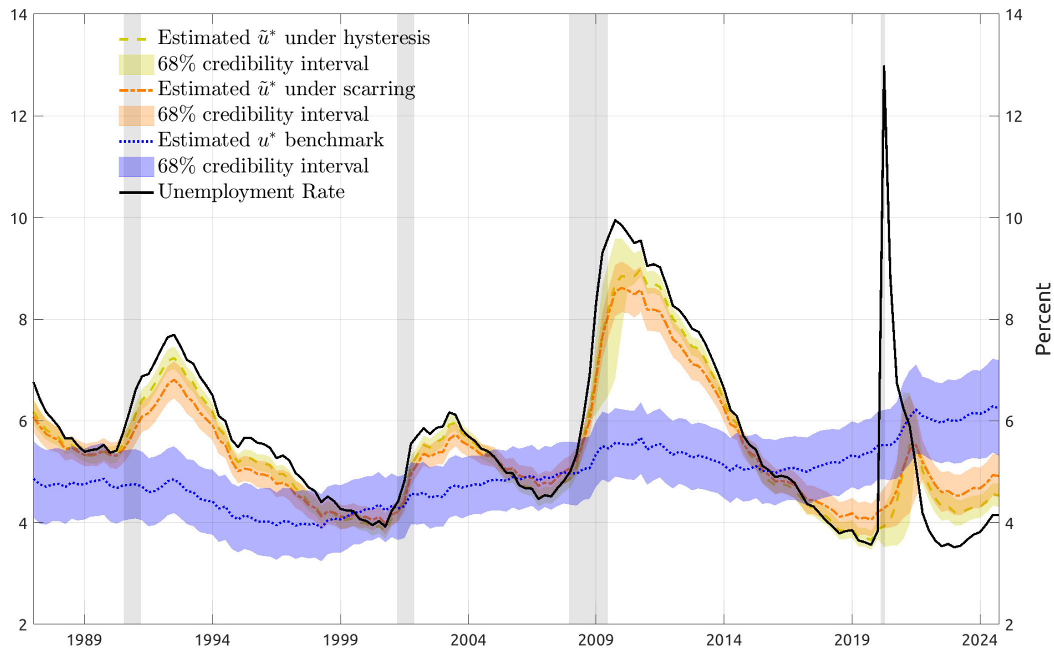

F A Model with Correlated Trend and Cycle Shocks

This appendix extends the scarring model by allowing for contemporaneous correlation between innovations to the cycle and innovations to the supply-driven output trend.

F.1 Specification

We relax the orthogonality assumption and allow

$$\mathrm{Corr}\left(\varepsilon_t, \eta_t^{y^*}\right) = \omega \neq 0, \tag{F.1}$$

where ε_t denotes the innovation to the cyclical component and $\eta_t^{y^*}$, the innovation to the supply-driven trend.

The law of motion for productive capacity remains

$$\tilde{y}_t^* = y_t^* + w_t^y, \tag{F.2}$$

with w_t^y evolving according to the scarring mechanism described in Section 3. Allowing for $\omega \neq 0$ introduces a contemporaneous link between permanent and transitory shocks, often interpreted as a time-to-build or adjustment effect (see Morley, Nelson and Zivot, 2003).

However, one could obtain correlated trend-cycle shocks in a reduced form by cyclical shocks affecting the trend (as in scarring or hysteresis), but also by trend shocks affecting the cycle. The latter mechanism could be the result of an IS-curve relationship in which the interest rate gap runs off a natural rate of interest which, in turn, is structurally a function of trend output growth and other shocks, such as preference disturbances. Laubach and Williams (2003) first adopt this formulation in a UC setup. We believe that this kind of structural formulation should be embedded in a UC model like the one proposed in this paper before adding correlated trend and cyclical shocks in a reduced-form way. We leave this addition for future research.

F.2 Results

Table F.1 reports posterior estimates when ω is freely estimated. The data favor a positive correlation between cyclical and trend innovations, similar to the results in González-Astudillo and Roberts (2022). Allowing for $\omega \neq 0$ does not materially change the scarring mechanism, as can be seen in the posterior estimates of both δ^y and δ^u.

Figures F.1—F.3 compare trend output, the cycle, and trend unemployment estimates between the scarring specification and the specification that adds correlated output trend-cycle shocks. As can be seen, the estimates of these latent variables are very similar between specifications, although the estimate of trend output in the specification that adds correlated output disturbances appears more uncertain than the baseline scarring specification.

Finally, we test with a Bayesian model comparison if the assumption of correlated disturbances is supported by the data. Figure F.4 shows the prior and posterior distributions of the correlation coefficient, ω, along with the probability that the scarring model with correlated trend and cycle disturbances be favored by the data, implied by the Savage-Dickey

Table F.1: Prior Distributions and Estimation Results — Correlated Shocks

		Scarring with Correlation		Scarring	
	Prior Dist.	Post. Mean	68% CI	Post. Mean	68% CI
ϕ_1	N(1.5,1)	1.09	[0.73,1.40]	1.25	[1.02,1.48]
ϕ_2	N(-0.6,1)	-0.14	[-0.45,0.21]	-0.30	[-0.52,-0.09]
θ_1	N(-0.35,0.25)	-0.44	[-0.58,-0.30]	-0.35	[-0.51,-0.19]
θ_2	N(-0.20,0.25)	-0.43	[-0.55,-0.31]	-0.47	[-0.61,-0.33]
β	N(0.7,0.5)	0.52	[0.42,0.62]	0.49	[0.38,0.61]
κ_1	N(0.1,0.5)	0.18	[0.08,0.28]	0.19	[0.08,0.31]
κ_2	N(0,0.5)	0.26	[0.08,0.42]	0.28	[0.10,0.46]
λ	N(-0.2,1)	-0.63	[-0.76,-0.49]	-0.65	[-0.79,-0.52]
β^w	N(0.8,0.5)	0.37	[0.27,0.46]	0.34	[0.23,0.46]
γ_1	N(-0.1,0.5)	-0.31	[-0.47,-0.14]	-0.36	[-0.61,-0.14]
γ_2	N(0,0.5)	-0.29	[-0.50,-0.07]	-0.31	[-0.53,-0.09]
ω	Beta(0,0.5)	0.42	[0.25,0.59]	0	—
y_0^*	N(911.9,5)	911.7	[910.3,913.0]	911.9	[910.5,913.5]
μ_0	N(1,1)	0.76	[0.63,0.90]	0.74	[0.61,0.88]
π_0^*	N(5,2)	4.88	[4.74,5.03]	4.88	[4.74,5.03]
u_0^*	N(5.9,2)	5.28	[4.54,6.02]	5.22	[4.50,5.93]
g_0^*	N(1.8,1)	1.78	[1.71,1.84]	1.77	[1.70,1.84]
κ		0.44	[0.24,0.63]	0.48	[0.23,0.71]
γ		-0.59	[-0.87,-0.32]	-0.67	[-0.99,-0.32]
$\rho^y = \delta^y$		0.56	[0.30,0.79]	0.58	[0.35,0.79]
$\rho^u = \delta^u$		0.46	[0.20,0.70]	0.47	[0.21,0.71]
max root AR(2)		0.93	[0.89,0.98]	0.91	[0.86,0.97]

Note: "N" stands for normal distribution where the first parameter is the mean and the second is the standard deviation. "Beta" denotes a Beta distribution where the first parameter is the mean and the second is the standard deviation.

Figure F.1: Productive Capacity with Correlation

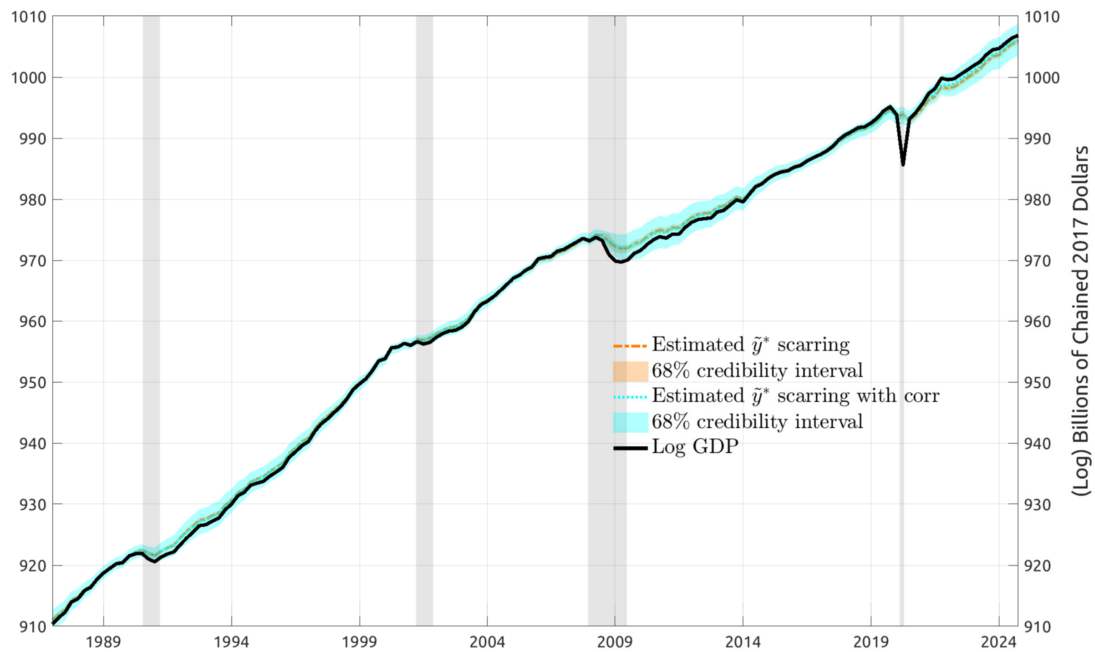

Figure F.2: Output Gap with Correlation

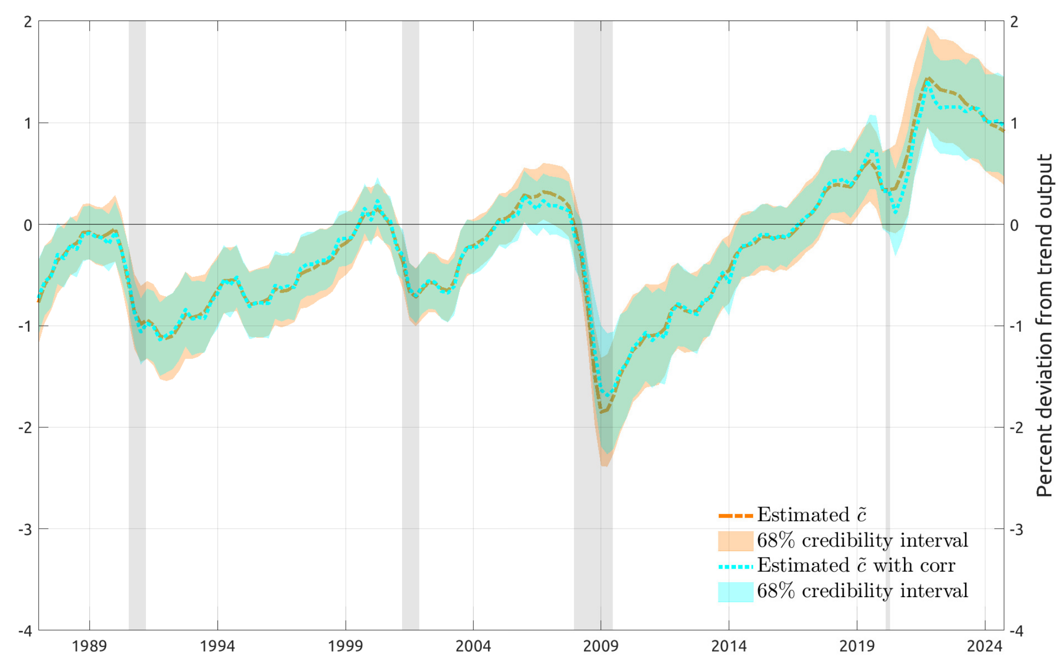

Figure F.3: Trend Unemployment with Correlation

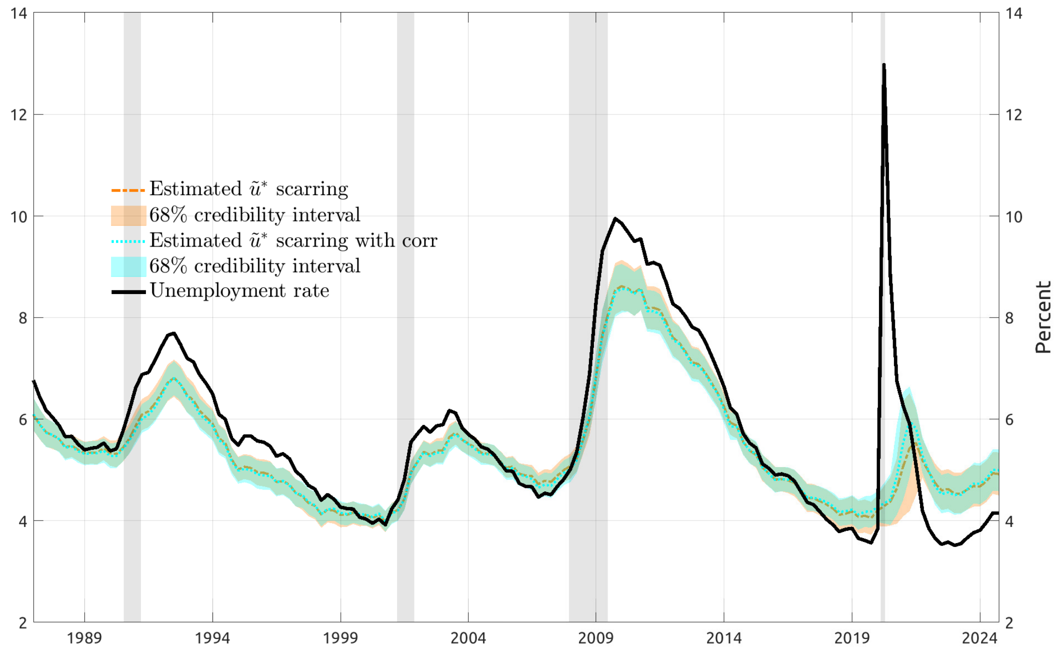

density ratio given by $BF_{s(\omega=0):s} = \frac{p(\omega=0|M_s)}{p(\omega=0|\text{data},M_s)}$. The results indicate that the model with correlated disturbances is more likely than not, given the data. Once again, we defer to further investigation if this correlation structure we find in a reduced-form setting can actually be picked up by more rich aggregate demand structure, such as an IS curve relationship that is absent in our setup.

Figure F.4: Savage-Dickey Density Ratio